

Bis-*N*-heterocyclic Carbene Palladium(IV) Tetrachloride Complexes: Synthesis, Reactivity, and Mechanisms of Direct Chlorinations and Oxidations of Organic Substrates

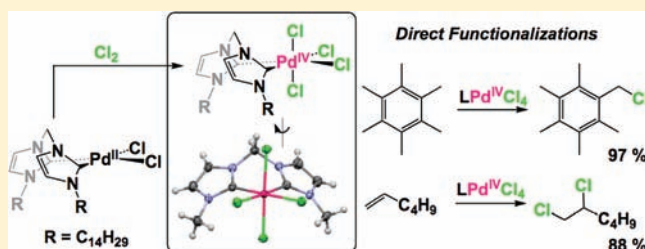
A. Scott McCall, Hongwang Wang, John M. Desper, and Stefan Kraft*

Department of Chemistry, Kansas State University, 213 CBC Building, Manhattan, Kansas 66506-0401, United States

S Supporting Information

ABSTRACT: This Article describes the preparation and isolation of novel octahedral CH₂-bridged bis-*N*-heterocyclic carbene)palladium(IV) tetrachlorides of the general formula LPd^{IV}Cl₄ [L = (NHC)CH₂(NHC)] from LPd^{II}Cl₂ and Cl₂. In intermolecular, nonchelation-controlled transformations LPd^{IV}Cl₄ reacted with alkenes and alkynes to 1,2-dichlorination adducts. Aromatic, benzylic, and aliphatic C–H bonds were converted into C–Cl bonds. Detailed mechanistic investigations in the dichlorinations of alkenes were conducted on the 18VE Pd^{IV}

complex. Positive solvent effects as well as kinetic measurements probing the impact of cyclohexene and chloride concentrations on the rate of alkene chlorination support a Pd^{IV}–Cl ionization in the first step. Product stereochemistry and product distributions from various alkenes also support Cl⁺-transfer from the pentacoordinated Pd^{IV}-intermediate LPd^{IV}Cl₃⁺ to olefins. 1-Hexene/3-hexene competition experiments rule out both the formation of π-complexes along the reaction coordinate as well as in situ generated Cl₂ from a reductive elimination process. Instead, a ligand-mediated direct Cl⁺-transfer from LPd^{IV}Cl₃⁺ to the π-system is likely to occur. Similarly, C–H bond chlorinations proceed via an electrophilic process with in situ formed LPd^{IV}Cl₃⁺. The presence of a large excess of added Cl[−] slows cyclohexene chlorination while the presence of stoichiometric amounts of chloride accelerates both Pd^{IV}–Cl ionization and Cl⁺-transfer from LPd^{IV}Cl₃⁺. ¹H NMR titrations, T₁ relaxation time measurements, binding isotherms, and Job plot analysis point to the formation of a trifurcated Cl[−] ··· H–C bond in the NHC-ligand periphery as a supramolecular cause for the accelerated chemical events involving the metal center.



INTRODUCTION

Palladium-mediated transformations have revolutionized organic chemistry over the past 30 years.¹ The main mode of operation in catalytic reactions involves Pd⁰/Pd^{II} cycles. However, in recent years, an alternative Pd^{II}/Pd^{IV} couple has been aggressively pursued in high-oxidation state routes that provide complementary reactivities unattainable to Pd⁰/Pd^{II} couples.² Two fields of particular interest in this arena focus on C–H bond activations/functionalizations and oxidative difunctionalizations of alkenes; under catalytic conditions, both of these reaction classes proceed through similar cycles involving a substrate activation step, an oxidation step, and a functionalization step (Scheme 1). A general paradigm has emerged that prescribes different roles for the metal in its oxidation states +2 and +4; specifically, activation steps that establish initial Pd–C bonds are executed by Pd^{II}, while functionalizations that establish C–X bonds are performed by Pd^{IV}.

The formation of the +4 oxidation state on palladium is often facilitated by the presence of strongly σ-donating carbon-ligands,³ and many isolable or spectroscopically characterized Pd^{IV} compounds are therefore organometallic in nature.⁴ However,

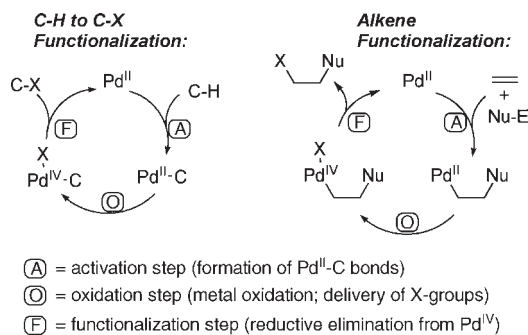
carbon-ligands on Pd^{IV} frequently do not constitute “spectator ligands” and become involved in reductive elimination events. Unlike square-planar Pd^{II}-analogues, octahedral d⁶ complexes of Pd^{IV} are not prone to unwanted side reactions such as β-eliminations,^{2a,b} and their reactivity is almost exclusively dominated by reductive eliminations;^{2d,3a,5} simple ligand substitutions⁶ as well as Pd^{IV} to M^{II} transmetalations (M^{II} = Pd^{II},^{5g,7} Pt^{II8}) represent the only exceptions. This narrow scope of Pd^{IV}-based transformations has effectively precluded the study of intermolecular Pd^{IV} chemistry with common organic functional groups. Another practical limitation in catalytic Pd^{II}/Pd^{IV} cycles is the common reliance on “chelation-controlled” or “ligand-directed” activations^{2e,9} by Pd^{II} to impart regioselectivity and to facilitate otherwise sluggish reactions.¹⁰

Novel direct Pd^{IV}-activations/functionalizations may provide an alternative to Pd^{II}/Pd^{IV} cycles that commonly require elevated reaction temperatures¹¹ to overcome barriers of rate-determining^{2b,c} Pd^{II} activation steps. Driven by an agenda to widen the scope of Pd^{IV} chemistry, we had to take on two tasks:

Received: August 26, 2010

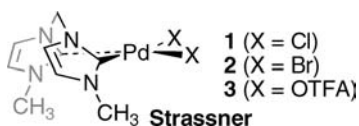
Published: January 19, 2011

Scheme 1



(i) provide a suitable nonreactive spectator ligand scaffold that can stabilize the metal center at its oxidation state +4 and (ii) identify intermolecular reaction types in which suitable groups are transferred from Pd^{IV} to substrates such as alkenes, alkynes, or aromatic platforms. In this work, we focused on studying stoichiometric Pd^{IV} reactions.

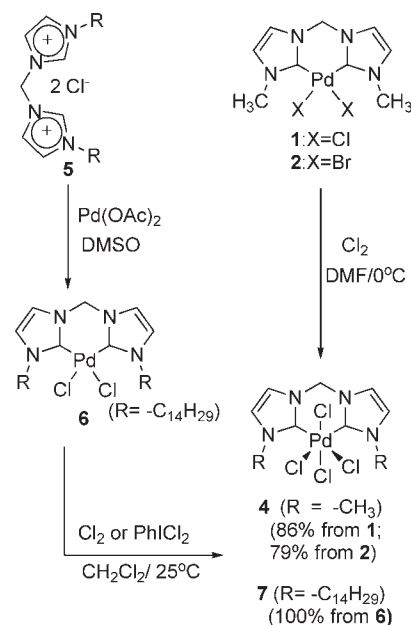
To address task (i), *N*-heterocyclic carbene ligands (NHCs)¹² appeared to be a suitable choice as ancillary support for Pd^{IV} due to their known propensity to stabilize highly oxidized metal centers without ligand dissociation.¹³ To this end, Arnold and Sanford recently demonstrated that a Pd^{IV}-NHC-dichloro-alkoxy-benzo[*h*]quinoline complex undergoes (benzo[*h*]quinoline)C-Cl reductive elimination with no C-Cl functionalization involving the NHC portion.¹⁴ It should be noted though that C-C reductive eliminations involving NHCs have occasionally been observed from NHC-Pd^{II}-methyl complexes.¹⁵ Given their ability to operate as catalysts for methane activation in strongly oxidizing milieu [K₂S₂O₈/(CF₃CO)₂O/CF₃COOH], we chose Strassner's bis-chelating NHC complexes LPd^{II}X₂ 1–3¹⁶ as a starting point for our explorations.



In addressing task (ii), we directed our initial efforts to the exploration of intermolecular reactions of Pd^{IV}-tetrahalides, in particular tetrachlorides. This choice was based on two criteria: (a) Tetrachloride complexes such as (bipy)PdCl₄¹⁷ and (en)-PdCl₄ and (py)₂PdCl₄ and [(NH₃)₄PdCl₂]₂Cl₂¹⁸ have been isolated previously and show limited thermal stability in the solid state. (b) The principal viability of C-H halogenations of hydrocarbons has been demonstrated in chelation-controlled Pd^{II}/Pd^{IV} cycles.¹⁹

Here, we report the synthesis and isolation of novel LPd^{IV}Cl₄ (L = NHC-CH₂-NHC) complexes and their stoichiometric intermolecular reactions with alkenes/alkynes as well as C-H bonds; neither alkenes nor alkynes have been previously reacted with isolated Pd^{IV} species of any kind. All substrates tested here are devoid of potential directing groups. Mechanistic studies on alkene dichlorinations revealed a stepwise process including initial Cl⁻ loss from the metal center and direct, ligand-mediated Cl⁺-transfer from LPd^{IV}Cl₃⁺ intermediates to π-bonds without the involvement of [LPd^{IV}Cl₃(η²-alkene)]⁺ complexes. Serendipitously, we discovered that C-H bonds of the NHC-ligand backbone in LPd^{IV}Cl₄ can act as hydrogen-bond

Scheme 2



donors toward added chloride ions to form supramolecular adducts of the type Cl⁻⋯(NHC)₂Pd^{IV}Cl₄. We discovered that these noncovalent interactions accelerate Pd^{IV}-Cl heterolysis to form a zwitterionic intermediate Cl⁻⋯(NHC)₂Pd^{IV}Cl₃⁺; we also found that Cl⁺-transfers from these intermediates to alkenes are accelerated in the presence of such C-H⋯Cl⁻ hydrogen bonds.

RESULTS

Synthesis of Pd^{IV} Tetrachlorides. The orange-yellow bis-chelating NHC-Pd^{IV} complex 4 was generated from a suspension of LPd^{II}Cl₂ complex 1^{16b} in DMF and Cl₂ in 86% yield (Scheme 2) and in 76% yield from LPd^{II}Br₂ complex 2. While poorly soluble in common organic solvents, we were able to obtain ¹H NMR spectroscopic data of 4 in DMF-*d*₇ with aromatic signals at δ 7.97, 7.80, two doublets for the bridging CH₂ group at δ 7.13, 6.85 (¹J = 13.1 Hz), and a CH₃ singlet δ 4.44. Similarly, the ¹³C NMR spectrum showed three ring signals at δ 139.08, 126.47, and 123.86 and a single peak for the bridging carbon at δ 63.42. ¹H and ¹³C NMR data are consistent with a C_s-symmetrical tub-shaped structure analogous to Pd^{II}-precursor 1.^{16b}

Vapor diffusion (DMF/CH₂Cl₂) produced crystals of 4 suitable for X-ray crystal structure analysis. In the solid state, the tetrachloride adopted an octahedral geometry around palladium (Figure 1). Pd-C^{carbene} bonds [Pd1-C32, 2.015(4) Å; Pd1-C22, 2.019(4) Å] experienced a bond lengthening of 0.046 and 0.049 Å as compared to 1,^{16b} hinting at diminished π-backbonding from a less π-basic d⁶-metal center.²⁰ Equatorial “in-plane” Pd-Cl^{eq} bond distances in 4 [Pd1-Cl1, 2.3769(10) Å; Pd1-Cl2, 2.3813(9) Å] remained almost unchanged relative to the Pd^{II}-precursor (Δ < 0.004 Å relative to 1) but were longer relative to their perpendicular Pd-Cl^{ax} counterparts [Pd1-Cl3, 2.3189(9) Å; Pd1-Cl4, 2.3081(9) Å] by an average of 0.066 Å, underlining a significant trans-influence of NHC ligands.

In an effort to bolster solubility in common organic solvents, tetradecyl-substituted bis-imidazolium dichloride 5 and Pd(OAc)₂ were converted to Pd(II) complex 6 as a white powder

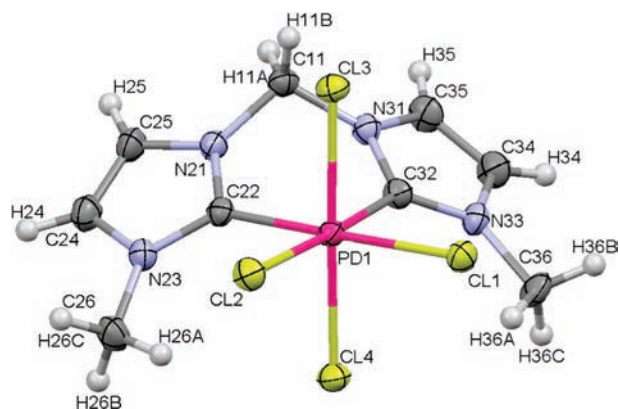
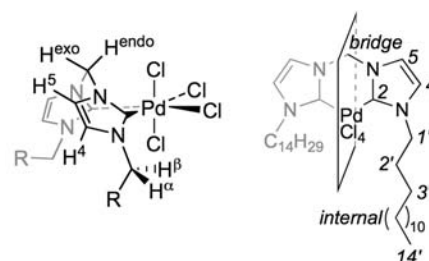


Figure 1. X-ray crystal structure of 4.

in 67% isolated yield (Scheme 2). Subsequent chlorination with $\text{Cl}_2/\text{CH}_2\text{Cl}_2$ yielded 7 as an orange-yellow powder quantitatively. Unfortunately, once 7 had precipitated from solution on the time scale of a few minutes, it remained insoluble in common organic solvents. We were able to obtain a ^1H NMR spectrum in CDCl_3 prior to the onset of precipitation via in situ chlorination of 6 and rapid spectral acquisition within 2 min. Two aromatic doublets at δ 8.32 and δ 7.08 (broad singlets) and two doublets (δ 7.48 and δ 7.07; $^2J = 13.4$ Hz) for the CH_2 -bridge were consistent with a tub-shaped C_s -symmetrical structure analogous to that of 4. Serendipitously, we discovered that the addition of the electrolytes Bu_4NCl or Bu_4NBF_4 dramatically increased the solubility of 7 in CDCl_3 , and up to 0.1 M solutions could be generated, which allowed for more time-consuming ^1H and ^{13}C NMR characterizations.²¹ We found that ^1H NMR chemical shifts of H^5 and H^{exo} experienced notable downfield shifts in $\text{CDCl}_3/\text{Bu}_4\text{NCl}$ by 0.37 and 1.34 ppm, respectively, relative to $\text{CDCl}_3/\text{Bu}_4\text{NBF}_4$ solutions, while their connected carbons C^5 and C^{bridge} were shifted upfield in the ^{13}C NMR spectrum by 0.51 and 0.61 ppm in $\text{CDCl}_3/\text{Bu}_4\text{NCl}$ (Figure 2).

A smaller upfield shift by 0.08 ppm was observed for H^4 , while C^4 was shifted downfield by 0.44 ppm. Electrolyte-dependent chemical shift differences for other protons and carbons were much less pronounced, and variations along the side chain faded out rapidly. Unambiguous assignments of all protons were accomplished via a $^1\text{H}-^1\text{H}$ ROESY experiment. Using $\text{H}^{\alpha,\beta}$ as a reference point, H^4 , H^5 , H^{exo} , and H^{endo} were identified through a chain of neighborhood relationships, giving rise to ROE cross-peaks of (H^4 , $\text{H}^{\alpha,\beta}$) and (H^5 , H^{exo}) as well as TOCSY-type cross-peaks for (H^5 , H^4) and (H^{exo} , H^{endo}) (Appendix 1, Supporting Information). Addition of other oxidants to bis-NHC-Pd^{II} complexes failed to produce stable Pd^{IV} products.^{22,23}

Chloride Binding Analysis. The remarkable impact of salts on the solubility of 7 in CDCl_3 prompted us to study their potential interactions with 7 in more detail. When ^1H NMR samples of 7 in $\text{CDCl}_3/\text{Bu}_4\text{NBF}_4$ were sequentially titrated with 0.1 equiv aliquots of Bu_4NCl , we were able to follow progressive downfield shifts for H^{exo} and H^5 and a progressive upfield shift for H^4 (Figure 3a), which was expected on the basis of the electrolyte-dependent chemical shifts of 7 (Figure 2). Notably, chemical shift changes leveled out with increasing concentrations of Bu_4NCl , which discredits the possibility of a bulk dielectric effect (Figure 3b). The Job plot²⁴ obtained from the ^1H NMR titration revealed a 1:1 binding ratio for $\text{Pd}^{\text{IV}}:\text{Cl}^-$ (Figure 4) for the new complex $7 \cdot \text{Cl}^-$. The equilibrium $7 + \text{Cl}^- \rightleftharpoons 7 \cdot \text{Cl}^-$



Proton	δ (Bu_4NBF_4)	δ (Bu_4NCl)	$\Delta\delta$
Hendo	7.12	6.94	-0.18
Hexo	6.83	8.17	+1.34
H ⁵	7.84	8.21	+0.37
H ⁴	7.10	7.02	-0.08
H ^{α/H^{β}}	4.86	4.81	-0.05
	4.73	4.68	-0.05

Carbon	δ (Bu_4NBF_4)	δ (Bu_4NCl)	$\Delta\delta$
2	139.10	138.63	-0.47
4	123.74	124.18	+0.44
5	122.83	122.32	-0.51
bridge	62.41	61.80	-0.61
1'	52.63	52.46	-0.17
2'	31.82	31.78	-0.04
3'	31.17	31.14	-0.03
14'	14.02	13.99	-0.03

Figure 2. ^1H and ^{13}C NMR chemical shifts for 7 in CDCl_3 in the presence of two different electrolytes (Bu_4NBF_4 and Bu_4NCl).

(Scheme 3) thermodynamically favors $7 \cdot \text{Cl}^-$, and from a Benesi-Hildebrand plot we obtained $K_{\text{eq}} = 139.2 \text{ M}^{-1}$ ($\Delta G_{\text{Cl}^-}^0 = -2.9$ kcal/mol).

For a structural localization of chloride binding, T1-relaxation studies were conducted for both 7 and $7 \cdot \text{Cl}^-$ (Figure 5). We found site-specific reductions in T1 values of $7 \cdot \text{Cl}^-$ relative to 7 by 25% and 17% for H^5 and H^{exo} , respectively, and an increase by 7% for H^4 , while other protons were virtually unaffected. Faster relaxation for H^5 and H^{exo} is consistent with the influence of enhanced $^{35}\text{Cl}/^{37}\text{Cl}$ -quadrupolar relaxations upon Cl^- -binding via a $\text{Cl}^- \cdots \text{H}-\text{C}$ hydrogen bond.²⁵

The combined data of chemical shift effects, NMR titration and Job plot, Benesi-Hildebrand analysis, and T1-relaxation times are in support of a trifurcated hydrogen bond in $7 \cdot \text{Cl}^-$ involving contacts of chloride to H^{exo} as well as H^5/H^4 in the ligand periphery (Scheme 3).

Reactivity. Small excesses (1.05 equiv) of $\text{LPd}^{\text{IV}}\text{Cl}_4$ (7 in $\text{Bu}_4\text{NBF}_4/\text{CDCl}_3$ or $7 \cdot \text{Cl}^-$ in $\text{Bu}_4\text{NCl}/\text{CDCl}_3$) were reacted at 25 °C with a variety of substrates including alkenes/alkynes as well as aromatic, benzylic, and aliphatic C-H bonds (Table 1). $\text{LPd}^{\text{IV}}\text{Cl}_2$ (6) was found to be the only organometallic product in all cases. Reaction conditions were not optimized, and yields were primarily limited by incomplete conversions (Table 1) rather than by the occurrence of uncharacterized side reactions. Alkenes/alkynes were converted into their 1,2-dichlorination adducts by $7 \cdot \text{Cl}^-$ (Table 1, entries 1-5) with side products from allylic and vinylic chlorinations (entries 3-5). Aromatic and benzylic C-H bonds of electron-rich substrates were converted into $\text{C}(\text{sp}^2)-\text{Cl}$ and $\text{C}(\text{sp}^3)-\text{Cl}$ bonds (entries 6-8, 10-11), while *p*-xylene was inert toward $7 \cdot \text{Cl}^-$ even upon

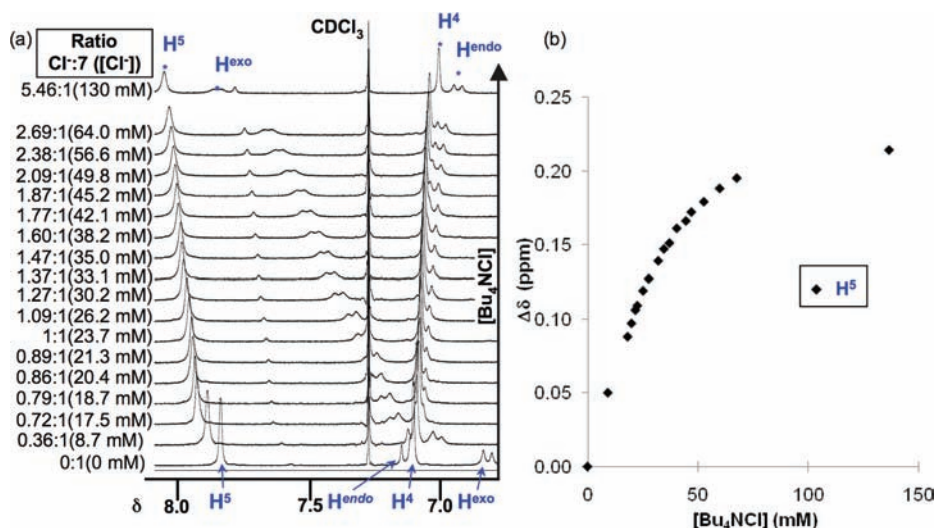


Figure 3. (a) ^1H NMR titration of **7** in $\text{CDCl}_3/\text{Bu}_4\text{NBF}_4$ with aliquots of Bu_4NCl displaying changes in chemical shifts of aromatic and bridge protons. (b) Saturation of chemical shift changes of H^5 at elevated Bu_4NCl concentration.

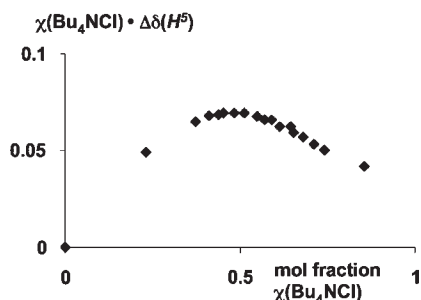


Figure 4. Job plot for mixtures of Bu_4NCl and $\text{LPd}^{\text{IV}}\text{Cl}_4$ (**7** and $7 \cdot \text{Cl}^-$ combined) in $\text{CDCl}_3/\text{Bu}_4\text{NBF}_4$ solutions. Plotted is $\chi(\text{Bu}_4\text{NCl}) \cdot \Delta\delta(\text{H}^5)$ as a function of $\chi(\text{Bu}_4\text{NCl})$ with $\chi(\text{Bu}_4\text{NCl}) = \text{mol fraction } [\text{Bu}_4\text{NCl}] / ([\text{Bu}_4\text{NCl}] + [\text{LPd}^{\text{IV}}\text{Cl}_4])$ and $\Delta\delta(\text{H}^5) = \delta(\text{H}^5)_{\text{max}} - \delta(\text{H}^5)$. A maximum at $\chi(\text{Bu}_4\text{NCl}) = 0.48$ is consistent with a 1:1 binding stoichiometry in complex $7 \cdot \text{Cl}^-$.

Proton	7		7·Cl⁻		ΔT1
	T1	(error)	T1	(error)	
H^5	1.179	(0.005)	0.887	(0.004)	-25%
H^4	1.066	(0.008)	1.144	(0.005)	+7%
H_{exo}	0.373	(0.003)	0.312	(0.007)	-17%
H_{endo}	0.492	(0.001)	0.456	(0.004)	-7%
$\text{H}^\alpha / \text{H}^\beta$	0.370	(0.001)	0.362	(0.001)	-2%
	0.371	(0.001)	0.364	(0.001)	-2%

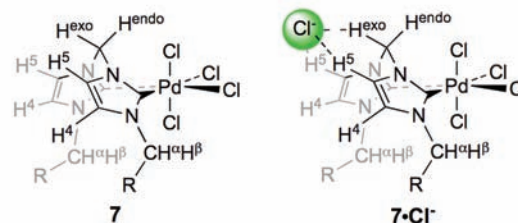
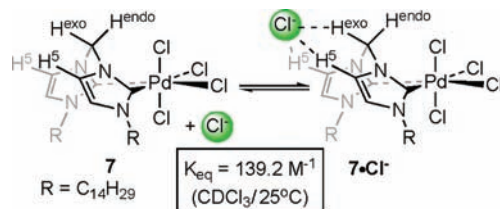


Figure 5. T1-relaxation studies of **7** and $7 \cdot \text{Cl}^-$.

Scheme 3



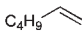
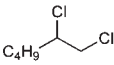
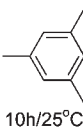
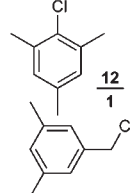

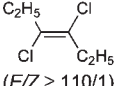
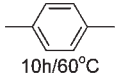
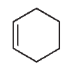
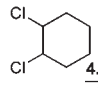
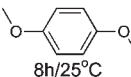
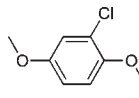
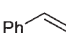
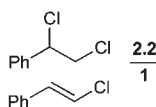
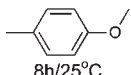
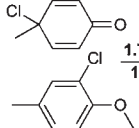
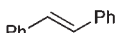
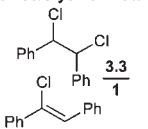
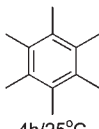
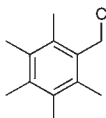
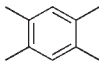
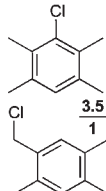
heating to 60°C . Methane was converted to methyl chloride, albeit in extremely low yield (entry 12). Methyl Grignard (entry 13) was oxidized to CH_3Cl and CH_3CH_3 , and bromide reacted with **7** to Br_2 (entry 14).

Alkene/alkyne dichlorinations in entries 2 and 3 showed predominant trans-selectivities in their 1,2-addition products, which matched selectivities obtained from electrophilic chlorinations with Cl_2 of identical substrates (Table 2). Equally, the three/erythro ratio (1.53/1) for 1,2-dichloro-1,2-diphenylethanes formed in the reaction of $7 \cdot \text{Cl}^-$ and stilbene (Table 1, entry 5) was nearly identical to the three/erythro ratio from the

respective Cl_2 -chlorination (Table 2). Furthermore, the abundance of side products from allylic chlorination (Table 1, entry 3) and vinylic chlorinations (Table 1, entries 4– and 5) was very similar to respective abundances in Cl_2 -chlorinations of cyclohexene, styrene, and stilbene (Table 2). This suggests the intermediacy of identical chloronium intermediates that determine stereochemistry and product distributions in chlorinations with Cl_2 and in chlorinations with $7 \cdot \text{Cl}^-$.

Mechanism of Alkene Chlorinations. General Considerations. We proceeded to elucidate the circumstances of Cl^+ -transfer from $\text{LPd}^{\text{IV}}\text{Cl}_4$ (**7** and $7 \cdot \text{Cl}^-$) to alkenes and alkynes. Three plausible reaction manifolds were considered (Scheme 4): In pathway 1, a direct, inner-sphere transfer of Cl^+ would occur directly between $\text{LPd}^{\text{IV}}\text{Cl}_4$ and an alkene or alkyne. Neutral species such as TiCl_3 ,²⁶ PbCl_4 ,²⁷ PCl_5 ,^{26b,28} SbCl_5 ,^{26b,29} MoOCl_4 ,³⁰ CrO_2Cl_2 ,³¹ or PhICl_2 ³² have previously been invoked in ionic Cl^+ -transfers to alkenes as reagents. Alternatively, $\text{LPd}^{\text{IV}}\text{Cl}_4$ may undergo concerted $\text{Cl}-\text{Cl}$ reductive elimination (pathway 2) followed by Cl_2 -chlorination of the alkene. Elimination

Table 1. Reactions of LPd^{IV}Cl₄ with Organic Substrates

LPd ^{IV} Cl ₄ +		Substrate	→	Product	+ LPd ^{II} Cl ₂		
Entry	Substrate Reaction Time/ Temperature/ Additive ^a	Product(s)/ Product Ratios ^b	% Total Yield (Conver- sion) ^c	Entry	Substrate Reaction Time/ Temperature/ Additive ^a	Product(s)/ Product Ratios ^b	% Total Yield (Conver- sion) ^c
1	 2h/25°C		88.8% (96.4%)	8	 10h/25°C	 12 / 1	69.5% (79.3%)
2	 1h/25°C	 (<i>E/Z</i> ≥ 110/1)	52.8% (59.1%)	9	 10h/60°C	No reaction	n.a.
3	 2h/25°C	 4.3 / 1	87.0% (87.0%)	10	 8h/25°C		70.8% (70.8%)
4	 2h/25°C	 2.2 / 1	87.4% (87.5%)	11	 8h/25°C	 1.7 / 1	98.1% (98.1%)
5	 1h/25°C	<i>threo/erythro</i> : 1.53/1  3.3 / 1	64.1% (64.1%)	12	CH ₄ ^d 2h/100°C	CH ₃ Cl ^e	2.9% (2.9%)
6	 4h/25°C		97.3% (97.3%)	13	CH ₃ MgBr ^f 2h/25°C	CH ₃ Cl ^e 1.1 / 1 CH ₃ CH ₃	34.3% (100%)
7		 3.5 / 1	54.5% (54.9%)	14	Bu ₄ NBr ^g	Br ₂ ^h	95.1% (100%)

^a Reaction conditions: 10–20 mM substrate; 150 mM Bu₄NCl/CDCl₃; 1.05 equiv of (freshly prepared) **7** unless otherwise noted. ^b Identified via ¹H NMR spectroscopy chemical shift analysis and compared to either authentic samples or published spectra (for references, see the Supporting Information). ^c Determined via ¹H NMR integration using 1,1,2,2-tetrachloroethane as an internal standard. ^d Headspace of a resealable J. Young NMR tube was purged with 1 atm of CH₄ prior to the reaction. ^e Volatiles were collected via flask-to-flask vacuum transfer using two J. Young NMR-tubes; ¹H NMR spectra were recorded and compared to the initial crude product mixture. ^f In THF-*d*₈ with a suspension of **7** under sonication in the absence of Bu₄NCl or Bu₄NBF₄. ^g 5 equiv of Bu₄NBr was reacted with **7**. ^h Identified and quantified after complete consumption of **7** by trapping with cyclohexene and quantifying the formed product 1,2-dibromocyclohexane and 3-bromocyclohex-1-ene via ¹H NMR spectroscopy.

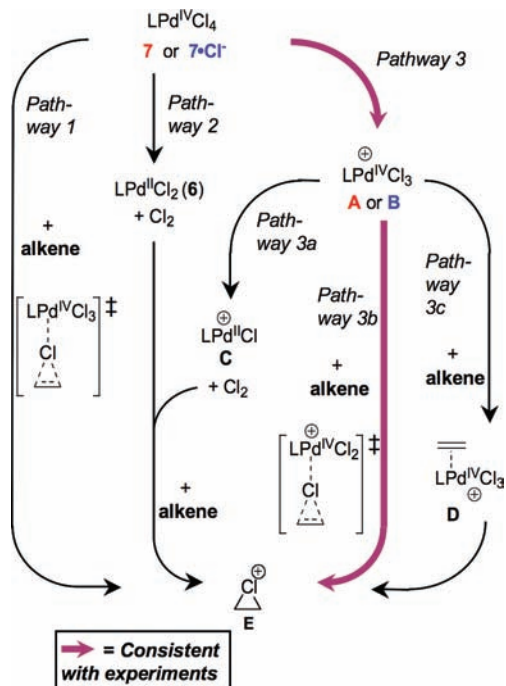
of Cl₂ is a common feature in inorganic complexes of Pd(IV)³³ such as (bipy)PdCl₄,¹⁷ Pd(NH₃)₂Cl₄,³⁴ Pd(py)₂Cl₄,³⁴ [Pd(NH₃)₄Cl₂]₂,³⁵ and Et₄N[PdCl₅(PPr₃)]³⁶ even though the precise mechanism of chlorine loss in these complexes is unknown.³⁷ In the ionic pathway 3, an initial loss of Cl[−] from LPd^{IV}Cl₄ would form ion pair **A** (from **7**) or zwitterionic analogue **B** (from **7** · Cl[−]; with intact Cl[−] ··· H–C hydrogen bonds on the ligand backbone). A reductive Cl₂ elimination from **A** or **B** may then form Pd^{II}-cation **C** while Cl₂ would act as the actual chlorinating

agent with the alkene (pathway 3a). Literature precedence for anion dissociation from octahedral Pd^{IV} complexes followed by reductive C–O and C–F eliminations was reported by Sanford^{6a} and Ritter.³⁸ Goldberg has established sequential ligand dissociations followed by reductive eliminations in octahedral platinum complexes.³⁹ Alternatively, we considered the possibility of a nucleophilic attack of the alkene to an electron-deficient Cl^{δ+}-ligand in intermediates **A** or **B** (pathway 3b). This would be reminiscent of reported S_N2-attacks of external nucleophiles on

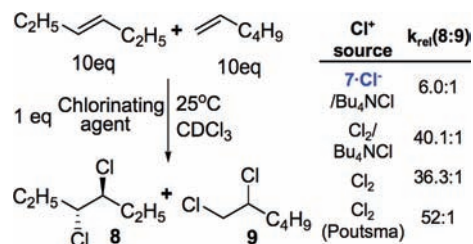
Table 2. Stereo- and Regioselectivity of Chlorination of Alkenes from Reactions with 7 as well as with Cl₂

Entry	Substrate	Products	Reaction Conditions and Product Ratios
1			7/Bu ₄ NCl ^a 4.3/1 Cl ₂ /Bu ₄ NCl ^b 6.6/1 Cl ₂ ^{c,d} 3-4/1
2			7/Bu ₄ NCl ^a 2.2/1 Cl ₂ /Bu ₄ NCl ^b 2.6/1 Cl ₂ ^e 5.7/1
3			7/Bu ₄ NCl ^a 1.53/1 Cl ₂ ^f 2/1
4			7/Bu ₄ NCl ^a >110/1 ^g Cl ₂ ^{h,i} 11.6/1

^a Solvent and salt additive identical to those described in Table 1. ^b 0.8 equiv of Cl₂ (saturated solution in CDCl₃) was rapidly added via syringe to a premixed solution of substrate in CDCl₃/Bu₄NCl. ^c Data from Poutsma, M. L. *J. Am. Chem. Soc.* **1965**, *87*, 2161–2171. ^d Reaction performed neat at 25 °C with the exclusion of light and in the presence of oxygen to eliminate the radical pathway. ^e Data from Iskra, J.; Stavber, S.; Zupan, M. *Chem. Commun.* **2003**, 2496–2497. ^f Data from Britsun, V. N.; Serguchev, Y. A.; Ganushchak, N. I. *Russ. J. Gen. Chem.* **2001**, *71*, 261–264. ^g (Z)-product was below detection limit by ¹H NMR spectroscopy. ^h Data from Heasley, G. E.; Coddling, C.; Sheehy, J.; Gering, K.; Heasley, V. L.; Shellhamer, D. F.; Rempel, T. *J. Org. Chem.* **1985**, *50*, 1773–1776. ⁱ Reaction performed in CH₂Cl₂.

Scheme 4


sp³-carbons of Pd^{IV}-C^{δ+} bonds.^{2d} Moreover, the transfer of Cl⁺ to alkenes has been reported for cationic species such as SbCl₄⁺,⁴⁰ PCl₄⁺,²⁸ and Cu^{II}Cl⁺.⁴¹ Last but not least, we considered the formation of Pd^{IV}(η²-alkene) complex D followed by chloropalladation (pathway 3c). Although spectroscopically identified Pd^{IV} π-complexes have not been reported in the literature


Figure 6. Relative rates (*k*_{rel}) for chlorination of 1-hexene and 3-hexene with 7·Cl⁻, Cl₂, and Cl₂/Bu₄NCl.

so far, calculations suggested that such species are energetically feasible.⁴² It should be noted that chloropalladations of alkenes or alkynes are known with Pd^{II}-chloride complexes.⁴³

Competition Experiments. In probing for the possibility of in situ formation of Cl₂ as the actual chlorinating agent in pathways 2 and 3a, (Scheme 4), we conducted a competition experiment in which 7·Cl⁻ was reacted with a 10 equiv/10 equiv mixture of 1-hexene and 3-*trans*-hexene in CDCl₃/Bu₄NCl; the resulting product ratio of 3,4-*trans*-dichlorohexane (8) and 1,2-dichlorohexane (9) was 6.0:1 (Figure 6). In contrast, we obtained a 40.1:1 ratio of 8 and 9 with Cl₂ as the chlorinating agent under otherwise identical conditions, which is close to Poutsma's ratio of 52:1 for Cl₂-chlorination of a neat mixture of 1-butene and 2-*trans*-butene.⁴⁴ The apparent mismatch between 7·Cl⁻ and Cl₂ in their internal versus terminal selectivities rules out the possibility of in situ formed Cl₂ from 7·Cl⁻ (pathways 2 and 3a). Furthermore, the 6.0:1 bias displayed by 7·Cl⁻ in the functionalization of the internal over the terminal hexane is at odds with the formation of η²-alkene complex C from B prior to chlorination in pathway 3c; metal complexes with terminal alkenes are generally more stable than complexes with internal alkenes,⁴⁵ and functionalizations of alkenes by Pd^{II} show higher rates for less substituted olefins.^{1,46}

Kinetic Experiments. To further elucidate the mechanism of Pd^{IV}-chlorinations, we conducted a series of individual kinetic measurements for the stoichiometric chlorinations of cyclohexene (cy) (Table 3, entries 1–24), styrene (styr) (entries 25–27), and hexamethylbenzene (HMB) (entry 28) as substrates in the reaction with 7 or 7·Cl⁻. The relative abundances of these two LPd^{IV}Cl₄ species were controlled in the equilibrium 7 + Cl⁻_{free} ⇌ 7·Cl⁻ by adjusting [Cl⁻]_{free}. Experimentally, we could only follow the disappearance of [7] and [7·Cl⁻] as a weighed average by ¹H NMR spectroscopy, and therefore we deliberately adjusted [Cl⁻]_{free} to levels that ensured a predominant abundance of either 7 or 7·Cl⁻. With relatively high chloride concentrations of [Cl⁻]_{free} ≥ 139 mM (entries 1–20 and 25–28), the major Pd^{IV} species in solution was 7·Cl⁻ (χ_{7·Cl⁻} ≥ 0.953); with relatively low chloride concentrations of [Cl⁻]_{free} ≤ 0.64 mM, compound 7 was predominant (χ₇ ≥ 0.920, entries 21–24). Upon inspection of entries 1–20 (reactions of cy with 7·Cl⁻) and entries 21–24 (reactions of cy with 7), it is apparent that measured values for *k*_{obs} are overall higher for 7·Cl⁻ than for 7 over a wide range of [cy]. At constant free chloride concentration ([Cl⁻]_{free} = 143 mM), higher concentrations of cyclohexene produce larger values for *k*_{obs} (entries 1–10). However, this relationship is not linear, and a plateau just above *k*_{obs} = 20 × 10⁻⁵ s⁻¹ is found for [cy] ≥ 300 mM (entries 1 and 2). A [cy] versus *k*_{obs} plot for entries 2–10 represents this saturation kinetics behavior graphically (Figure 3, top).⁴⁷ Qualitatively, styrene displays similar plateau characteristics in its

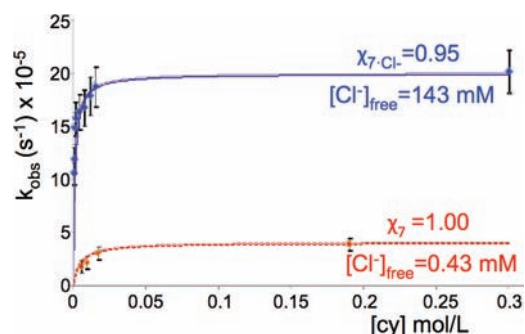
Table 3. Observed Rates for the Chlorination of Cyclohexene, Styrene, and Hexamethylbenzene with 7 and 7·Cl⁻ at Various Substrate and Chloride Concentrations

entry	substrate ^a	[substrate] (mM)	[Cl ⁻] _{free} (mM) ^b	mol fraction 7·Cl ⁻ ($\chi_{7\cdot\text{Cl}^-}$) ^c	$k_{\text{obs}} \times 10^{-5}$ (s ⁻¹) ^d
1	cy	608	143	0.954	20.2 ± 0.3
2	cy	300	143	0.954	20.2 ± 0.2
3	cy	15.0	143	0.954	18.8 ± 0.2
4	cy	11.3	143	0.954	17.9 ± 0.3
5	cy	7.20	143	0.954	16.8 ± 0.3
6	cy	3.60	143	0.954	16.4 ± 0.3
7	cy	1.50	143	0.954	15.8 ± 0.5
8	cy	0.58	143	0.954	14.9 ± 0.5
9	cy	0.29	143	0.954	11.9 ± 0.6
10	cy	0.14	143	0.954	10.6 ± 0.9
11	cy	3.43	151	0.957	16.6 ± 0.1
12	cy	120	313	0.981	19.5 ± 0.7
13	cy	3.46	313	0.981	11.8 ± 0.3
14	cy	2.77	313	0.981	8.8 ± 0.2
15	cy	0.44	688	0.993	7.6 ± 0.3
16	cy	0.37	688	0.993	6.9 ± 0.5
17	cy	0.32	688	0.993	5.2 ± 0.8
18	cy	0.28	688	0.993	5.9 ± 0.6
19	cy	0.25	688	0.993	4.5 ± 0.4
20	cy	0.23	688	0.993	3.1 ± 0.2
21	cy	190	0.47	0.060	5.1 ± 0.2
22	cy	16.7	0.64	0.080	4.6 ± 0.1
23	cy	9.07	0.34	0.045	3.1 ± 0.1
24	cy	5.36	0.43	0.055	2.8 ± 0.1
25	styr	300	166	0.962	22.5 ± 0.4
26	styr	210	166	0.962	23.3 ± 0.5
27	styr	14.4	166	0.962	12.7 ± 0.2
28	HMB	38.9	139	0.953	22.2 ± 0.8

^a Substrates in the table are listed as cy = cyclohexene, styr = styrene, and HMB = hexamethylbenzene. ^b For entries 1–20 and 25–28, the concentration of free chloride ([Cl⁻]_{free}) was determined by subtracting the amount of hydrogen-bonded Cl⁻ (within 7·Cl⁻) from the total chloride concentration [Cl⁻]_{total} in the system (from added Bu₄NCl). In entries 15–18, small amounts of chloride were present as a 1:1 byproduct from allylic chlorination of cyclohexene. [Cl⁻]_{total} was then derived from the ¹H NMR integral of RRC(Cl)H of 3-chloro-cyclohexene. The hydrogen-bonded chloride portion within 7·Cl⁻ was subtracted from [Cl⁻]_{total} to determine [Cl⁻]_{free}. ^c Derived from 7 + Cl⁻_{free} ⇌ 7·Cl⁻ ($K_{\text{eq}} = 139.2 \text{ M}^{-1}$); see Supporting Information eq 12 and the Supporting Information chapter “Kinetic Analysis and Rate Law Derivation” for details. ^d Rates for disappearances of 7 and 7·Cl⁻ were determined by ¹H NMR spectroscopy. Errors were calculated using ANOVA regression analysis to a 95% confidence interval and given as the standard error for each measurement

reaction with 7·Cl⁻ (entries 25–27), and k_{obs} levels out at approximately $23 \times 10^{-5} \text{ s}^{-1}$.

Adding extra Pd^{II} complex 6 (LPd^{II}Cl₂) to the solutions of cyclohexene or styrene did not affect their k_{obs} values, which excludes that Pd^{II}(alkene) complexes may play a role as a reactive intermediate during the reaction. We generated only one data point for the chlorination of hexamethylbenzene (HMB, entry 28) with 7·Cl⁻, and it matches the k_{obs} plateau values of cyclohexene and styrene [$k_{\text{obs}}(\text{HMB}) = 22.2 \times 10^{-5} \text{ s}^{-1}$]. Qualitatively, the reaction of 7 (entries 21–24) with cyclohexene

**Figure 7.** Saturation kinetics plots for the chlorination of cyclohexene with 7 (bottom line, dashed) and 7·Cl⁻ (top line, contiguous).

follows a saturation kinetics trend similar to 7·Cl⁻; however, the k_{obs} plateau value of approximately $5 \times 10^{-5} \text{ s}^{-1}$ is about 5 times lower for 7 (Figure 7, bottom line) than for 7·Cl⁻.⁴⁸

While the addition of chloride ions can increase k_{obs} through shifting the equilibrium 7 + Cl⁻_{free} ⇌ 7·Cl⁻ toward the side of the more reactive 7·Cl⁻, a large excess of [Cl⁻]_{free} has a detrimental outcome on k_{obs} . This effect reveals itself in entries 6 and 13 with virtually identical cyclohexene concentration ([cy] = 3.60 mM and 3.46 mM); a higher free chloride concentration in entry 13 decreases the observed rate constant ([Cl⁻]_{free} = 313 mM, $k_{\text{obs}} = 11.8 \times 10^{-5} \text{ s}^{-1}$) as compared to an environment with a lower free chloride concentration in entry 6 ([Cl⁻]_{free} = 143 mM, $k_{\text{obs}} = 16.4 \times 10^{-5} \text{ s}^{-1}$). The rate suppression in entry 13 is observed despite a slight increase in the relative abundance of the more reactive species 7·Cl⁻ in entry 13 ($\chi_{7\cdot\text{Cl}^-} \geq 0.981$) as compared to entry 6 ($\chi_{7\cdot\text{Cl}^-} \geq 0.954$). Increasing [Cl⁻]_{free} to 688 mM depressed k_{obs} even further (entries 15–20), and the emergence of an inverse relationship between [Cl⁻]_{free} and k_{obs} becomes apparent when comparing entries 15 and 20.

Quantitative Kinetic Analysis. Taken together, the saturation kinetics in [cy] versus k_{obs} , the chloride-dependent depressions of k_{obs} at high [Cl⁻]_{free} and low [cy], as well as the chemoselective chlorination of internal versus terminal alkenes are at odds with pathways 1, 2, 3a, and 3c (Scheme 4), but consistent with pathway 3b for both Pd^{IV} complexes 7 and 7·Cl⁻. Next, we took on the task of extracting quantitative data pertaining to the elementary steps in pathway 3b. First, we describe the overall disappearance of the total amount of Pd^{IV} ([Pd^{IV}] = [7] + [7·Cl⁻]) as:

$$\frac{d[\text{Pd}^{\text{IV}}]}{dt} = -k_{\text{obs}}[\text{Pd}^{\text{IV}}] \quad (1)$$

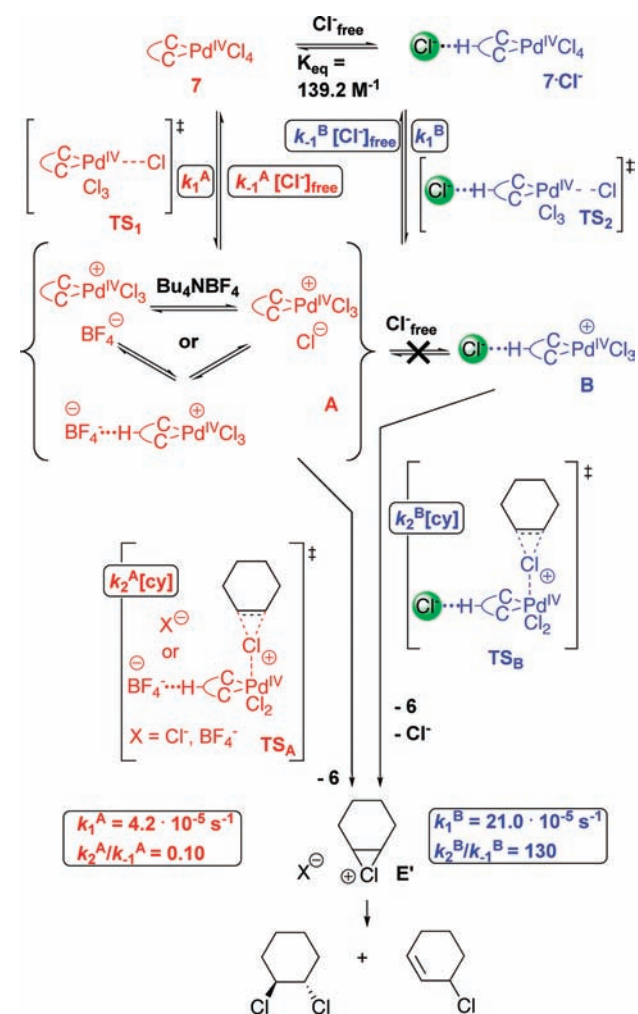
Our analysis is based on a rapid pre-equilibrium between 7 and 7·Cl⁻ in the presence of free chloride ions (7 + Cl⁻_{free} ⇌ 7·Cl⁻).⁴⁹ Furthermore, we define k_7 and $k_{7\cdot\text{Cl}^-}$ as first-order observed rate constants for the disappearance of 7 and 7·Cl⁻ (eq 2a,b). Essentially, k_7 and $k_{7\cdot\text{Cl}^-}$ mimic the role of observable rate constants, even though our experimental technique of data collection (¹H NMR spectroscopy) only provides for average signals of 7 and 7·Cl⁻. Combining eq 1 and eq 2a,b yields eq 3.

$$\frac{d[7]}{dt} = -k_7[7] \text{ and } \frac{d[7\cdot\text{Cl}^-]}{dt} = -k_{7\cdot\text{Cl}^-}[7\cdot\text{Cl}^-] \quad (2a,b)$$

$$\frac{d[\text{Pd}^{\text{IV}}]}{dt} = -(k_7[7] + k_{7\cdot\text{Cl}^-}[7\cdot\text{Cl}^-]) \quad (3)$$

Combining eqs 1 and 3 and expressing the abundance of [7] and [7·Cl⁻] within [Pd^{IV}] through individual mole fractions χ_7

Scheme 5



and $\chi_{7 \cdot \text{Cl}^-}$ ($[7] = \chi_7[\text{Pd}^{\text{IV}}]$ and $[7 \cdot \text{Cl}^-] = \chi_{7 \cdot \text{Cl}^-}[\text{Pd}^{\text{IV}}]$) provides eq 4.

$$k_{\text{obs}} = \chi_7 k_7 + \chi_{7 \cdot \text{Cl}^-} k_{7 \cdot \text{Cl}^-} \quad (4)$$

Equation 4 manifests the additive approach to k_{obs} , which is separated into individual reactivities of 7 and 7·Cl⁻ as well as their respective abundances. This simple concept necessitates that once intermediate A is formed from 7, it cannot directly equilibrate with B on the time scale of the Cl⁺-transfer from A to cyclohexene.⁵⁰ Experimental evidence will be presented (vide infra) in support of such slow ion pair dynamics.

Scheme 5 lays out the conceptual framework for multistep reactions including absolute rate constants for the elementary steps. It is based on the equilibrium between 7 and 7·Cl⁻. Chloride dissociation from the metal centers in 7 and 7·Cl⁻ is described through k_1^A and k_1^B , while k_{-1}^A and k_{-1}^B are rate constants for the microscopic reverse chloride addition to intermediates A and B. Furthermore, bimolecular Cl⁺-transfers from A and B to cyclohexene to form E' are expressed through k_2^A and k_2^B . No intermediates were detected in the reactions of 7 and 7·Cl⁻ with cyclohexene (nor with any other substrate), and we apply a steady-state model for A and B. On the basis of this approach, eq 4 turns into a "bimodal" expression (eq 5) whose two components constitute individual

"steady-state" terms for the interplay of 7 and A (first addend) as well as 7·Cl⁻ and B (second addend) (for detailed derivations, see the Supporting Information).

$$k_{\text{obs}} = \chi_7 \frac{k_1^A [\text{cy}]}{\left(\frac{k_{-1}^A}{k_2^A}\right) [\text{Cl}^-]_{\text{free}} + [\text{cy}]} + \chi_{7 \cdot \text{Cl}^-} \frac{k_1^B [\text{cy}]}{\left(\frac{k_{-1}^B}{k_2^B}\right) [\text{Cl}^-]_{\text{free}} + [\text{cy}]} \quad (5)$$

Four limiting scenarios can be discussed in the context of eq 5:

- (i) $[\text{Cl}^-]_{\text{free}} > [\text{Pd}^{\text{IV}}]$, $k_{-1}^B/k_2^B[\text{Cl}^-]_{\text{free}} \ll [\text{cy}]$. In this case, one obtains $\chi_{7 \cdot \text{Cl}^-} \approx 1$, $\chi_7 \approx 0$, and k_{obs} is reduced to the rate constant k_1^B for chloride dissociation from 7·Cl⁻ (eq 6). This scenario reflects the plateau level for the saturation kinetics of 7·Cl⁻ (Figure 3, top), in which case the initial ionization of 7·Cl⁻ is rate determining.

$$k_{\text{obs}} = k_1^B \quad (6)$$

- (ii) $[\text{Cl}^-]_{\text{free}} \ll [\text{Pd}^{\text{IV}}]$, $k_{-1}^A/k_2^A[\text{Cl}^-]_{\text{free}} \ll [\text{cy}]$. In this case, one obtains $\chi_{7 \cdot \text{Cl}^-} \approx 0$, $\chi_7 \approx 1$, and k_{obs} is reduced to the rate constant k_1^A for chloride dissociation from 7 (eq 7). This scenario reflects the plateau level for the saturation kinetics of 7 (Figure 3, bottom) in which case the initial ionization of 7 is rate determining.

$$k_{\text{obs}} = k_1^A \quad (7)$$

- (iii) $[\text{Cl}^-]_{\text{free}} \gg [\text{Pd}^{\text{IV}}]$, $k_{-1}^B/k_2^B[\text{Cl}^-]_{\text{free}} \gg [\text{cy}]$. In this case, one obtains $\chi_{7 \cdot \text{Cl}^-} \approx 1$, $\chi_7 \approx 0$, and k_{obs} can be expressed according to eq 8. In this case, k_{obs} is proportional to [cy] and inversely proportional to $[\text{Cl}^-]_{\text{free}}$. In chemical terms, this refers to a scenario in which 7·Cl⁻ and B are effectively part of a pre-equilibrium and the rate-determining step is the transfer of Cl⁺ to cyclohexene.

$$k_{\text{obs}} = \frac{k_1^B k_2^B}{k_{-1}^B} \frac{[\text{cy}]}{[\text{Cl}^-]_{\text{free}}} \quad (8)$$

Experimentally determined rates of disappearance of 7·Cl⁻ in the presence of very low concentrations of cyclohexene ($[\text{cy}] = 0.14\text{--}0.44 \text{ mM}$, $[\text{Cl}^-]_{\text{free}} = 143 \text{ mM}$, 688 mM) (entries 10, 15–20, Table 3) produced a linear relationship when plotting $\ln(k_{\text{obs}})$ versus $\ln([\text{cy}]/[\text{Cl}^-]_{\text{free}})$ (Figure 8). A slope of 0.97 confirmed the anticipated first-order dependence on $[\text{cy}]/[\text{Cl}^-]_{\text{free}}$.

The inverse rate dependence on $[\text{Cl}^-]_{\text{free}}$ can be explained in chemical terms through a rate-determining transfer of Cl⁺ from B to cyclohexene; the pre-equilibrium $7 \cdot \text{Cl}^- \rightleftharpoons \text{B} + \text{Cl}^-_{\text{free}}$ is shifted to the left by increasing $[\text{Cl}^-]_{\text{free}}$. The switch in rate-determining step as compared to scenario (i) is brought about by a decrease of the $[\text{cy}]/[\text{Cl}^-]_{\text{free}}$ ratio.

- (iv) $[\text{Cl}^-]_{\text{free}} \ll [\text{Pd}^{\text{IV}}]$, $k_{-1}^A/k_2^A[\text{Cl}^-]_{\text{free}} \gg [\text{cy}]$. We were not able to explore this domain as practical concentrations of

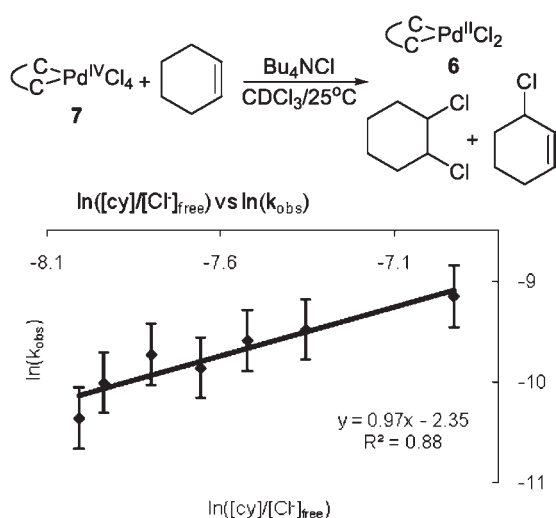


Figure 8. Rates of chlorination of cyclohexene with $7 \cdot \text{Cl}^-$ (from **7** and Bu_4NCl) at extremely low $[\text{cy}]:[\text{Cl}^-]_{\text{free}}$ ratios (1:1000–1:3000) with a slope ~ 1 in the \ln/\ln plot.

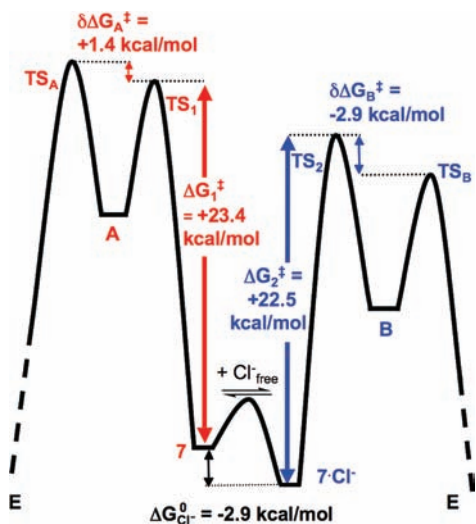


Figure 9. Energy diagram for the reactions of $\text{LPd}^{\text{IV}}\text{Cl}_4$ (**7** and $7 \cdot \text{Cl}^-$) with cyclohexene to form chloronium intermediate **E** via $\text{LPd}^{\text{IV}}\text{Cl}_3^+$ intermediates **A** and **B**. Represented are enthalpies of ionization (ΔG_1^\ddagger and ΔG_2^\ddagger) as well as the enthalpic differences between Cl^- transfer from $\text{LPd}^{\text{IV}}\text{Cl}_3^+$ to cyclohexene and Cl^- return to $\text{LPd}^{\text{IV}}\text{Cl}_3^+$ ($\delta\Delta G_A^\ddagger$ and $\delta\Delta G_B^\ddagger$).

cyclohexene would have to be significantly lower than in scenario (iii), in which case $[\text{cy}]$ had been only slightly above our ^1H NMR detection limit.

Simulations. To quantitatively determine values of k_1^A , k_1^B , as well as (k_2^A/k_{-1}^A) and (k_2^B/k_{-1}^B) , we simulated experimental results using cks-software,⁵¹ which uses a stochastic algorithm⁵² and therefore serves for an analytical treatment of Scheme 5 that is independent of the validity of eq 5 and eqs 6–8 from scenarios (i), (ii), and (iii). We iteratively modeled the disappearances of starting materials **7** and $7 \cdot \text{Cl}^-$ with the concentrations and conditions provided in Table 3 (entries 1, 3–10, 15, 16, 17, and 18). We were able to obtain a reasonable and comprehensive fit for all entries with the adjustable parameters set to: $k_1^A = 4.2 \times$

10^{-5} s^{-1} ($\Delta G_A^\ddagger = +23.4 \text{ kcal mol}^{-1}$) (Figure 9), $k_1^B = 21.0 \times 10^{-5} \text{ s}^{-1}$ ($\Delta G_B^\ddagger = +22.5 \text{ kcal mol}^{-1}$), $k_2^A/k_{-1}^A = 0.10$ ($\delta\Delta G_A^\ddagger = +1.4 \text{ kcal mol}^{-1}$), and $k_2^B/k_{-1}^B = 130$ ($\delta\Delta G_B^\ddagger = -2.9 \text{ kcal mol}^{-1}$).⁵³ Together with the already established value $\Delta G_{\text{Cl}^-}^0 = -2.9 \text{ kcal mol}^{-1}$ for the equilibrium $7 + \text{Cl}^-_{\text{free}} \rightleftharpoons 7 \cdot \text{Cl}^-$, these values are the basis for an energy diagram, featuring a lower barrier for $\text{Pd}^{\text{IV}}\text{–Cl}$ heterolysis in $7 \cdot \text{Cl}^-$ than in **7** ($\Delta G_A^\ddagger - \Delta G_B^\ddagger = +0.9 \text{ kcal/mol}$) (Figure 9). It also underscores the rather small energetic differences between TS_1 and TS_A as well as TS_2 and TS_B , allowing for the observation of $[\text{cy}]$ -dependent saturation kinetics. The interconversion of **7** and $7 \cdot \text{Cl}^-$ is too rapid on the NMR time scale to spectroscopically distinguish between them as a result of a low energetic barrier between them [$\Delta G(\text{exchange}) \leq +14.0 \text{ kcal mol}^{-1}$ for exchange of hydrogen-bonded chloride in $7 \cdot \text{Cl}^-$ with external $\text{Cl}^-_{\text{free}}$ via formation of intermediate **7**].⁵⁴

Values for k_1^A , k_1^B , k_2^A/k_{-1}^A , and k_2^B/k_{-1}^B from cks-simulations were then entered into eq 5 to generate simulation plots for k_{obs} at particular chloride concentrations (Figure 7). For $[\text{Cl}^-]_{\text{free}} = 143 \text{ mM}$, the k_{obs} simulation plot is represented with a contiguous line (Figure 7, top); in this case, the major Pd^{IV} component in solution was $7 \cdot \text{Cl}^-$. For $[\text{Cl}^-]_{\text{free}} = 0.43$, the k_{obs} simulation plot is represented with a dashed line (Figure 7, bottom); in this case, the major Pd^{IV} component in solution was **7**. Both simulation plots are in good agreement with experimental k_{obs} data in Figure 7.

Solvent Effect. Solvent effects were investigated in the reactions of cyclohexene with **7** in $\text{CDCl}_3/\text{Bu}_4\text{NBF}_4$ and **4** in $\text{DMF-}d_7$.⁵⁵ While not mapping out a complete kinetic profile for **4** in $\text{DMF-}d_7$, we were able to obtain a pseudofirst-order rate constant [$k_{\text{obs}}(\text{DMF-}d_7) = (214 \pm 13) \times 10^{-5} \text{ s}^{-1}$] with respect to **4** (23.6 mM), while the $[\text{cy}] = 472 \text{ mM}$. At such high cyclohexene concentration, it is reasonable to assume that $k_{\text{obs}}(\text{DMF-}d_7)$ solely reflects the chloride dissociation step (k_1) from the metal and $k_{\text{obs}}(\text{DMF-}d_7) = k_1(\text{DMF-}d_7)$. In comparing this value to $k_1^A = 4.2 \times 10^{-5} \text{ s}^{-1}$ (measured in $\text{CDCl}_3/\text{Bu}_4\text{NBF}_4$ in the absence Cl^-), we obtain the relative rate $k_{\text{rel}} = k_1(\text{DMF-}d_7):k_1^A = 51:1$.

Reaction with Aromatic Substrates. Various electron-rich aromatic substrates reacted with $7 \cdot \text{Cl}^-$, causing ring and benzylic chlorinations in good yields (Table 1, entries 6–8, 10, 11), while *p*-xylene was inert even upon heating to 60 °C for 10 h (entry 9). 4-Methylanisole was chlorinated in its 2- and 4-positions yet not in the 3-position (entry 11), 1,4-dimethoxybenzene was smoothly converted to 2-chloro-1,4-dimethoxybenzene, hexamethylbenzene underwent benzylic chlorination (entry 6), while mesitylene (entry 8) and durene (entry 7) were functionalized in both ring and benzylic positions. We followed the reaction of hexamethylbenzene and $7 \cdot \text{Cl}^-$ by ^1H NMR spectroscopy and found a substrate-independent rate law $d[7 \cdot \text{Cl}^-]/dt = k_{\text{obs}}[7 \cdot \text{Cl}^-]$ with $k_{\text{obs}} = 22.2 \times 10^{-5} \text{ s}^{-1}$ (CDCl_3 , 25 °C, Table 2), which matched the rate constant for chloride dissociation from $7 \cdot \text{Cl}^-$ ($k_1^B = 21.0 \times 10^{-5} \text{ s}^{-1}$) reasonably well. In contrast, bimolecular rate laws $d[7 \cdot \text{Cl}^-]/dt = k_{\text{bi}}[7 \cdot \text{Cl}^-][\text{substrate}]$ were observed for 4-methylanisole ($k_{\text{bi}} = 2.1 \times 10^{-3} \text{ M}^{-1} \text{ s}^{-1}$) and dimethoxybenzene ($k_{\text{bi}} = 6.1 \times 10^{-3} \text{ M}^{-1} \text{ s}^{-1}$).

Reaction of $7 \cdot \text{Cl}^-$ with Methane and Side-Chain Chlorination. We were able to react CH_4 with $7 \cdot \text{Cl}^-$ at elevated temperatures to produce CH_3Cl in small quantities (entry 12, Table 1). While a relatively low CH_4 pressure ($p_{\text{CH}_4} = 1 \text{ atm}$) may have prevented higher yields, we found predominant intramolecular chlorination of the $\text{C}_{14}\text{H}_{29}$ -chain of $7 \cdot \text{Cl}^-$. Reacting $7 \cdot \text{Cl}^-$ in the absence of organic substrates with excess

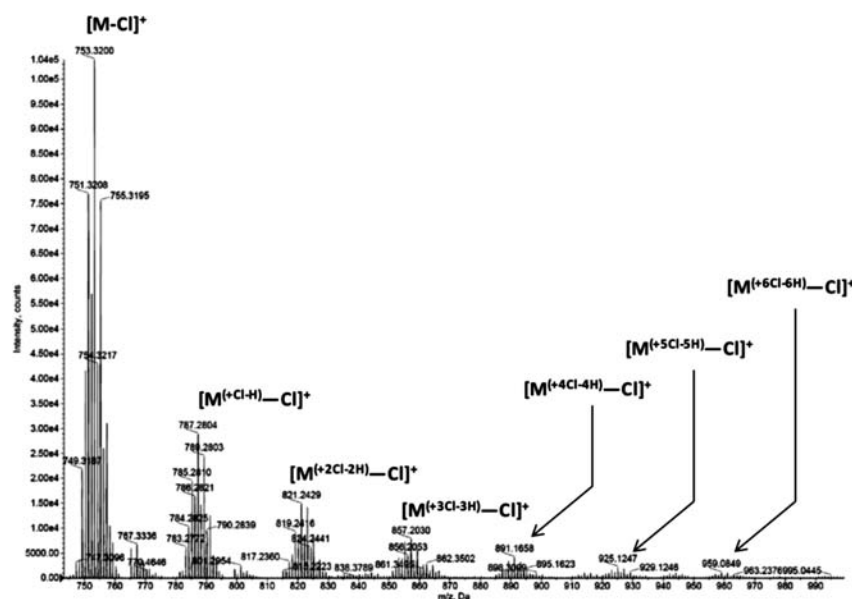


Figure 10. Mass spectrum of chlorination products ($\text{LPd}^{\text{IV}}\text{Cl}_3^+$) from the reaction of **7** with excess Cl_2 . Up to six H/Cl substitution events within the ligand could be identified.

Cl_2 produced multiple chlorination events in the side chain, when exposed to 1 atm Cl_2 at 25 °C for 16 h with the exclusion of light, presumably via a catalytic $\text{Pd}^{\text{II}}/\text{Pd}^{\text{IV}}$ cycle. The occurrence of up to six substitutions of C–H bonds with C–Cl bonds in $\text{LPd}^{\text{IV}}\text{Cl}_4$ was confirmed by MS(ESI) spectroscopy (Figure 10). A control experiment using hexane in $\text{CDCl}_3/\text{Bu}_4\text{NCl}$ solution and Cl_2 showed no aliphatic chlorination products over the same period.

Reaction with Bromide. In an attempt to initiate Cl/Br ligand substitution in $\text{LPd}^{\text{IV}}\text{Cl}_4$, we reacted a suspension of **7** (1 equiv) in CDCl_3 with Bu_4NBr (5 equiv). Within seconds, the yellow solid decolorized and dissolved. An ^1H NMR analysis showed the quantitative formation of $\text{LPd}^{\text{IV}}\text{Br}_2$ complex **6**. The oxidation of Br^- gave rise to Br_2 , which was confirmed by adding cyclohexene (1 equiv) and identifying the adducts 1,2-dibromocyclohexane and 3-bromocyclohexene by ^1H NMR and ESI–MS spectroscopy.

DISCUSSION

Synthesis and Properties of $\text{LPd}^{\text{IV}}\text{Cl}_4$ Complexes. The facile and clean conversion of $\text{LPd}^{\text{II}}\text{Cl}_2$ to $\text{LPd}^{\text{IV}}\text{Cl}_4$ was accomplished with Cl_2 or PhICl_2 as oxidants. This method has been used in the past to synthesize tetrachlorides (bipy)- PdCl_4 ¹⁷ and (en) PdCl_4 and (py)₂ PdCl_4 and $[(\text{NH}_3)_4\text{PdCl}_2]\text{Cl}_2$.¹⁸ In contrast, the bromination of $\text{LPd}^{\text{II}}\text{Br}_2$ complex **2** produced a new material whose formation was apparently driven by precipitation rather than by intrinsic driving forces because we observed facile Br_2 loss to regain **2**. The reaction of $\text{LPd}^{\text{IV}}\text{Cl}_4$ complex **7** with Br^- produced Br_2 and $\text{LPd}^{\text{II}}\text{Cl}_2$ complex **6** rather than engaging in Br^-/Cl^- ligand substitutions (entry 14, Table 1). Given that the formation of bis-NHC– Pd^{IV} bromides seems to be thermodynamically unfavorable in solution, we were able to exploit these properties by Cl_2 oxidation of Pd^{II} dibromide **2** (which is synthetically more easily accessible than Pd^{II} dichloride **2**) to $\text{LPd}^{\text{IV}}\text{Cl}_4$ product **4** with complete loss of Br^- ligands. Our attempts to synthesize oxygenated complexes of the type $\text{LPd}^{\text{IV}}(\text{OR})_n\text{Cl}_m$ ($m+n=4$) met with failure when a variety of peroxides failed to convert starting materials. This failure is

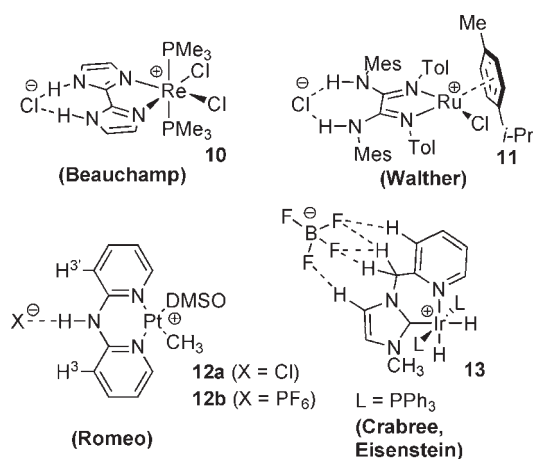
mirrored by the absence of any isolable tetraoxygenated Pd^{IV} complexes in the literature. The X-ray crystal structure of **4** reveals an isomorphous relationship to the tub-shaped bis-NHC chelate in square planar Pd^{II} precursor **1**.^{16b} Interestingly, the $\text{Pd}-\text{C}^{\text{carbene}}$ bonds were lengthened by 0.046 and 0.049 Å relative to the same bonds in **1**, while $\text{Pd}-\text{Cl}^{\text{eq}}$ bonds on the opposite site were virtually unaltered in their bond lengths ($\Delta < 0.004$ Å). We attribute the $\text{Pd}-\text{C}^{\text{carbene}}$ bond lengthening to a decrease in π -backbonding.⁵⁶ The existence of $d-\pi^*$ interactions is in line with a growing literature consensus on the general viability of π -backbonding in metal–NHC complexes.^{20,57} Furthermore, NHC ligands are known to exert a strong trans-influence on metal–ligand bonds in the trans position;⁵⁸ inspection of $\text{Pd}-\text{Cl}$ bond lengths in **4** corroborates this trend with longer equatorial in-plane $\text{Pd}-\text{Cl}^{\text{eq}}$ bonds as compared to shorter, unaffected axial $\text{Pd}-\text{Cl}^{\text{ax}}$ bonds ($\Delta_{\text{average}} = 0.066$ Å). The longer $\text{Pd}-\text{C}^{\text{carbene}}$ bonds in **4** relative to **1** (diminished backbonding) paired with virtually no bond length differences for $\text{Pd}-\text{Cl}^{\text{eq}}$ in both **4** and **1** (unaltered trans-influence) underscores that π -backbonding and trans-influence are independent effects that have no significant synergistic relationship. This conclusion is consistent with the premise that trans-influences are transmitted primarily through the σ -framework of a coordination compound.⁵⁹

A unique structural feature of CH_2 -bridged bis-NHC complexes is the nearly collinear alignment of the three $\text{C}-\text{H}^{\text{exo}}$ and $\text{C}-\text{H}^{\text{exo}}$ bonds (Figure 1; see C25–H25, C35–H35, C11–H11A). Through a series of experiments including ^1H NMR titrations of Cl^- and T1 relaxation measurements, we established that these three C–H bonds could act as hydrogen-bond donors toward chloride ions to form supramolecular adduct **7**· Cl^- .

Halide binding to purely organic receptors has been reported. For example, imidazolium cations are prone to form hydrogen bonds with halides,⁶⁰ Flood found that neutral C–H hydrogen-bond donors from macrocyclic triazolophanes were able to hydrogen bond Cl^- to a total of eight C–H bonds of the host with binding enthalpies in CD_2Cl_2 of up to -9.6 kcal mol⁻¹ with an average of -1.2 kcal mol⁻¹

per $\text{Cl}^- \cdots \text{H}-\text{C}$ bond.⁶¹ In comparison, the trifurcated hydrogen-bonding interaction in $7 \cdot \text{Cl}^-$ ($\Delta G_{\text{Cl}^-}^0 = -2.9 \text{ kcal mol}^{-1}$) amounts to $-0.97 \text{ kcal mol}^{-1}$ per hydrogen bond. However, it should be pointed out that the binding interaction of **7** and Cl^- could only be determined in the presence of Bu_4NBF_4 to dissolve **7** in the first place. It is therefore conceivable that **7** and BF_4^- anions engage in weak hydrogen-bonding contacts by themselves and addition of Cl^- simply causes a binding competition. Therefore, $\Delta G_{\text{Cl}^-}^0$ may constitute a relative binding affinity, and its value of $-2.9 \text{ kcal mol}^{-1}$ would therefore have to be regarded as a conservative lower limit. Interestingly, this hydrogen-bonding contact in the periphery of $7 \cdot \text{Cl}^-$ affects its chemical reactivity in comparison to the parent compound **7**.

Related transition metal complexes capable of hydrogen bonding anions to the periphery of the ligand scaffold have been previously published by Beauchamp,⁶² Walther,⁶³ Romeo,⁶⁴ as well as Crabtree and Eisenstein⁶⁵ in compounds **10–13**; these interactions include $\text{Cl}^- \cdots \text{H}-\text{N}$ hydrogen bonds (**10–12**) and “carbon-based” $\text{F}_3\text{BF}^- \cdots \text{H}-\text{C}$ hydrogen bonds in iridium complex **13**. However, complexes **10–13** are all based on cationic metal centers, and hydrogen bonds merely supplement underlying electrostatic interactions within each ion pair. To the best of our knowledge, $7 \cdot \text{Cl}^-$ constitutes the first reported Cl^- -adduct to a neutral transition metal complex, with possible electrostatic interactions only to the counteranion Bu_4N^+ .



Reactivity. The reactivity of **7** toward a variety of functional groups was studied (Table 1). Reactions were run in the presence of an excess of chloride (150 mM Bu_4NCl in CDCl_3), and therefore the predominant Pd^{IV} species in solution was $7 \cdot \text{Cl}^-$ rather than **7**. Alkenes and alkynes were chlorinated to 1,2-dichlorinated products; *E/Z* product ratios as well as side products from allylic and vinylic chlorinations with cyclohexene, styrene, and stilbene mirror results from chlorinations of identical alkenes/alkynes with Cl_2 under electrophilic conditions (Table 2). These matching outcomes suggest a stepwise mechanism involving the formation of organic chloronium intermediates that subsequently react via trans-addition of Cl^- or via proton loss to produce vinylic and allylic chlorination side products. To understand the transfer of Cl^+ from $\text{LPd}^{\text{IV}}\text{Cl}_4$ to π -systems, we studied the reaction of **7** and $7 \cdot \text{Cl}^-$ with alkenes in more detail. Interactions of isolated Pd^{IV} compounds with alkenes or alkynes have never been studied, even though the existence of $(\eta^2\text{-alkene/alkyne})\text{Pd}^{\text{IV}}$ complexes was proposed in Heck reactions^{42,66} and other carbopalladations,⁶⁷ allylic C–H acetoxylation,⁶⁸ and cyclotrimerizations.⁶⁹

Mechanism of Alkene Chlorinations. We considered three fundamental pathways that included direct bimolecular Cl^+ -transfer from $\text{LPd}^{\text{IV}}\text{Cl}_4$ to the olefin (pathway 1, Scheme 4), loss of Cl_2 from $\text{LPd}^{\text{IV}}\text{Cl}_4$ (for example, via concerted reductive elimination) and subsequent alkene chlorination by Cl_2 (pathway 2), and, last, Cl^- -dissociation from $\text{LPd}^{\text{IV}}\text{Cl}_4$ to form cation $\text{LPd}^{\text{IV}}\text{Cl}_3^+$ (pathway 3). For the latter, we considered reductive elimination of Cl_2 from $\text{LPd}^{\text{IV}}\text{Cl}_3^+$ (pathway 3a); alternatively, a direct Cl^+ -transfer from $\text{LPd}^{\text{IV}}\text{Cl}_3^+$ to the alkene was contemplated (pathway 3b). A third plausible variation was seen in the involvement of π -coordinated intermediates $\text{LPd}^{\text{IV}}\text{Cl}_3$ - $(\eta^2\text{-alkene})^+$ (**D**) prior to intra- or intermolecular chloropalladation (pathway 3c).

Saturation Kinetics. In determining the relationship between alkene concentration and k_{obs} , we investigated the disappearance of $\text{LPd}^{\text{IV}}\text{Cl}_4$ during its reaction with cyclohexene (Table 3). In controlling the concentration of free chloride⁷⁰ ($[\text{Cl}^-]_{\text{free}}$), we were able to set the concentrations of **7** and $7 \cdot \text{Cl}^-$ and arrive at predominant abundances of either species **7** ($\chi \geq 0.92$) at low $[\text{Cl}^-]_{\text{free}}$ or $7 \cdot \text{Cl}^-$ ($\chi \geq 0.954$) at high $[\text{Cl}^-]_{\text{free}}$. Saturation kinetics behavior was independently found for both species at different plateau levels (Figure 7). Such plateau domains for $[\text{cy}]$ -independent k_{obs} values rule out a strictly bimolecular process according to pathway 1 (Scheme 4) but would be consistent with stepwise pathways 2 and 3. At sufficiently high $[\text{cy}]/[\text{Cl}^-]_{\text{free}}$ ratios ≥ 2 , we observe a unimolecular rate law $d[7 \cdot \text{Cl}^-]/dt = k_{\text{obs}}[7 \cdot \text{Cl}^-]$, and the rate is independent of $[\text{Cl}^-]_{\text{free}}$. However, at very low ratios $[\text{cy}]/[\text{Cl}^-]_{\text{free}} < 1/1500$, we were able to manifest a domain with $d[7 \cdot \text{Cl}^-]/dt \propto 1/[\text{Cl}^-]_{\text{free}}$. Rate suppressions by $[\text{Cl}^-]_{\text{free}}$ would not be expected for pathway 2 but are supportive of pathway 3 with a rate-determining loss of metal-bound chloride in the initial step followed by fast Cl^+ -transfer to cyclohexene. At low $[\text{cy}]/[\text{Cl}^-]_{\text{free}}$ ratios, we are promoting the addition of $\text{Cl}^-_{\text{free}}$ to the metal center in **B** at the expense of the forward reaction of **B** and cyclohexene. In other words, the initial dissociation of $7 \cdot \text{Cl}^-$ into **B** and $\text{Cl}^-_{\text{free}}$ becomes reversible on merits of relative abundances of $\text{Cl}^-_{\text{free}}$ over cy . Comparing unimolecular plateau rates of compound **7** in $\text{CDCl}_3/\text{Bu}_4\text{NBF}_4$ ($d[7]/dt = k_{\text{obs}}[7]$) with unimolecular conversions of **4** in DMF-d_7 ,⁷¹ we found a 51-fold rate acceleration in the more polar solvent.⁷² Again, such an effect would not be expected for pathway 2 with a rate-determining Cl_2 loss from $7 \cdot \text{Cl}^-$, while rate-determining ionization (pathway 3) is fully consistent with a positive solvent effect.

Competition Experiment. Further insight the nature of the conversion of an alkene into a chloronium intermediate was sought. Even under conditions that render the initial step (Cl_2 loss in pathway 2 or Cl^- -dissociation in pathway 3) rate determining, a competition experiment between two alkenes with distinct degrees of substitutions would provide meaningful relative rates for the alkene functionalization step. In reacting $7 \cdot \text{Cl}^-$ with a 10 equiv/10 equiv mixture of 1-hexene/3-hexene, we found a 6:1 bias for chlorination of the internal over the terminal alkene, which did not match with the bias that free Cl_2 displayed under identical conditions (40.1:1). This finding excludes pathways that rely on in situ formed Cl_2 as the active chlorinating agent (pathways 2 and 3a). By the same token, we interpret the 6:1 preference of $7 \cdot \text{Cl}^-$ in favor of the more substituted alkene as an indication against a process involving π -complexes $\text{LPd}^{\text{IV}}\text{Cl}_3(\eta^2\text{-alkene})^+$. Although no mechanistic

studies on potentially existing Pd^{IV} π -complexes have been reported so far, a plethora of reactions in the literature involving migratory insertions^{46a,b} of alkenes into Pd^{II}–R bonds corroborate our chemoselectivity argument; for example, rates of Heck reactions slow with an increasing degree of alkene substitution^{1,46c,d} and Pd^{II}-based carbopalladations,^{46e–g} hydro-palladations,^{46h,i} as well as aminopalladations show identical trends.^{46j–l} Most important, the Pd^{II}–Cl addition across isoprene showed kinetic chloropalladation of the less substituted C=C bond.^{46m,n} The generally higher reactivity of Pd^{II} complexes toward terminal alkenes in metal-mediated reactions is at odds with the intermediacy of LPd^{IV}Cl₃(η^2 -alkene)⁺ (C) in pathway 3c. In contrast, in ligand-mediated alkene transformations, such as dichlorinations by CrO₂Cl₂⁷³ as well as OsO₄-catalyzed dihydroxylations,⁷⁴ functional groups are directly installed on the C=C bond without prior π -coordination to the metal. Ligand-mediated transformations prefer electron-rich internal alkenes and are less sensitive toward steric factors.^{73b} Equally, electrophilic alkene functionalizations with three-membered transition states, such as epoxidations or halogenations, also display a strong preference for internal alkenes.^{73b,75} A picture emerges in which chloronium intermediate is formed via a ligand-mediated transfer of Cl⁺ from an intermediate LPd^{IV}Cl₃⁺ (A or B, depending on the precursor 7 or 7·Cl[−]) to the alkene; from the viewpoint of the alkene, this reaction may be considered an “S_N2-type” attack to a Cl-ligand in A or B. While our reactions have not been extended to catalytic applications yet, it is apparent that these direct Pd^{IV}-based alkene functionalizations diverge from the paradigm in Scheme 1 in which Pd^{II} and a O⁷⁶-, N^{46j,77}-, or C⁷⁸-nucleophile are added across the olefin in the activation⁷⁹ step followed by Pd^{II}/Pd^{IV} oxidation^{6b,19a,80} and the C–X bond-forming event (“functionalization”) on the oxidation state +4; LPd^{IV}Cl₄ has the ability to bypass otherwise necessary interactions between the olefin and Pd^{II}.

Supramolecular Catalysis in the Pd^{IV}–Cl Dissociation Step. In Scheme 5, we summarize our conclusion of a two-step chlorination mechanism; the opening event involves Cl[−]-dissociation from LPd^{IV}Cl₄ via polarized transition states TS₁ and TS₂. The resulting intermediates A and B subsequently transfer Cl⁺ to the alkene in a ligand-mediated process (TS_A and TS_B). Dynamic simulations of kinetic data from Table 3 allowed us to extract rate constants for Pd^{IV}–Cl heterolyses in 7 (k_1^A) and in 7·Cl[−] (k_1^B), and we found that k_1^B is about 5 times larger than k_1^A and the barrier height difference $\Delta G_B^\ddagger - \Delta G_A^\ddagger$ amounts to −0.9 kcal/mol. We propose that the formation of a positive charge on the metal center in transition state TS₁ energetically benefits from the proximity of an adjacent negative charge that is held in place by a supramolecular contact. Effectively, the role of Cl[−] is that of a catalyst; attachment of chloride to the ligand periphery facilitates the detachment of chloride from the metal. This is noteworthy because electrostatic supramolecular catalysis in which nearby ionic guests affect the reactivity of neutral hosts through space is rarely seen with organic molecules⁸¹ and is unprecedented for transition metal complexes. The higher reactivity of 7·Cl[−] over 7 can also be explained by a special salt effect⁸² in which externally added anions or cations affect the reactivity of a system through specific interactions.⁸³ In compound 7·Cl[−], the chloride ion from the electrolyte heteroconjugates⁸⁴ to the neutral receptor 7 via hydrogen bonding and addition of chloride ions to 7 creates a nonlinear rate increase as 7·Cl[−] is formed until 7 is consumed. The specific 1:1 binding

of chloride and 7, the higher reactivity of 7·Cl[−] over 7, and the nonlinearity of this rate acceleration expose our system as a rare case of a specific salt effect on a neutral molecule.

Effect of Chloride on the Distribution Factor k_2/k_{-1} . An interesting facet of the kinetic analysis is the 1300-fold reversal of distribution factors ($k_2^A/k_{-1}^A = 1:10$ and $k_2^B/k_{-1}^B = 130:1$) that reflect the inherent preference of LPd^{IV}Cl₃⁺ (A and B) for Cl⁺-transfer to cyclohexene as compared to Cl[−]-addition to the metal center. Because short-lived intermediates A and B could not be directly detected by ¹H NMR spectroscopy, structural proposals can only be putative. As far as intermediate B is concerned, we propose a zwitterionic supramolecular structure based on the fact that hydrogen-bonded chloride lowers the barrier for loss of metal bound chloride, and it is therefore likely that Cl[−] experiences an even stronger association with the cation LPd^{IV}Cl₃⁺ than with LPd^{IV}Cl₄. Furthermore, the conversion of B to 7·Cl[−] is kinetically dependent on [Cl[−]]_{free}. The need for an attack of external chloride ions to B is consistent with a structure of B containing an immobilized, hydrogen-bonded Cl[−] that is unavailable for an internal return reaction.⁸⁵ Structurally related ion pairs that bind Cl[−] via hydrogen bonds in their ligand periphery have been isolated by others (compounds 10–12). The in situ formation of a cationic Pd^{IV} centers in chloroform has been recently described by Sanford;^{6a} we propose that factors contributing to the relative ease of formation of B include: (a) a relatively tight zwitterionic constellation involving the counteranion; (b) the presence of two strongly σ -donating carbene ligands;¹³ and (c) the presence of π -donating chloride ligand.⁸⁶

Our understanding of the structure of A is more vague. Heterolysis of a Pd^{IV}–Cl bond in 7 is likely to initially produce an intimate ion pair LPd^{IV}Cl₃⁺Cl[−], which may subsequently react with external BF₄[−] via an exchange pathway based on (−/+/−) triple ions⁸⁷ to establish BF₄[−]···H–C hydrogen bonds on the periphery of the ligand similar to structure 13⁶⁵ and analogous to the proposed structure of B.⁸⁸ Altering the anion environment from BF₄[−] for A to Cl[−] for B has a noticeable impact on their relative reactivities k_2/k_{-1} that diverge 1300 fold for k_2^A/k_{-1}^A and k_2^B/k_{-1}^B . This is in contrast to Romeo’s observation that the reactivities toward DMSO exchange of 12a,b (as well as analogues with X = OTf, BF₄) are virtually unaffected by the nature of the counterion.⁶⁴ The explanation for different reactivities of A and B may lie in different proximities between cation LPd^{IV}Cl₃⁺ to the counteranion X within X[−]···(NHC)₂Pd^{IV}Cl₃⁺ given the differences in ionic radii of Cl[−] (1.81 Å)⁸⁹ and BF₄[−] (2.20 Å).⁹⁰ Consequently, the effective positive charge on the metal center may be more pronounced in A and may enhance charge-controlled reactivity (Cl[−]-capture) over orbital control with the neutral substrate cyclohexene. Variations in the degree of charge separation have been frequently invoked in the literature to explain reactivity differences in inorganic and organometallic ion pairs.⁹¹

Irrespective of the chemical preferences of A and B, their reluctance to interconvert into each other on the time scale of their reactions with cyclohexene (“forward reaction”) and chloride (“return reaction”) is remarkable in light of the often very rapid intra- and intermolecular ion pair dynamics on the time scale of 100–400 ps.⁹² Mechanistically, fast intermolecular ion exchange channels, even in nonpolar solvents, involve the formation of triple ions⁸⁷ or quadrupoles.⁹³ However, Romeo found that X = PF₆[−]/Cl[−] exchange between 12b and 12a proceeds comparatively slowly ($k_2 = 96 \text{ M}^{-1} \text{ s}^{-1}$; $\Delta G^\ddagger = 14.9 \text{ kcal mol}^{-1}$). Based on a bimolecular rate law, this suggested a

“direct bimolecular attack by the chloride on the acidic proton to remove the less tightly bound hexafluorophosphate ion” as opposed to a conventional triple ion or quadrupole pathway. We suggest that the reluctance of **A** to convert into **B**, even in the presence of free chloride ions, has kinetic impediments similar to those found in **12a,b**.

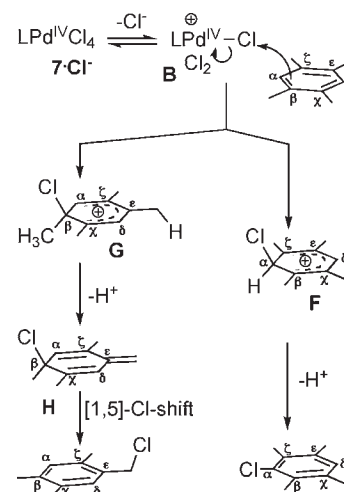
Reaction of B with Aromatic π -Systems. Expanding our scope from isolated alkenes to aromatic π -systems, we discovered that $\text{LPd}^{\text{IV}}\text{Cl}_4$ complex $7 \cdot \text{Cl}^-$ produced aromatic and benzylic chlorination products, and we found evidence for the interaction of $\text{LPd}^{\text{IV}}\text{Cl}_3^+$ intermediate **B** with aromatic substrates reminiscent of pathway 3b for the chlorination of alkenes (Scheme 4). Chlorinations of aromatic substrates by $7 \cdot \text{Cl}^-$ both on the ring as well in benzylic positions (if available) were possible with electron-rich substrates (Table 1, entries 7, 8, 10, 11), while xylene (entry 9) was inert even at 60 °C. This is consistent with an electrophilic delivery of Cl^+ by **B**. In line with this is the observed regioselectivity in the chlorination of 4-methylanisole in its 2- and 4-positions (entry 11) consistent with the reported reactivity of this substrate in electrophilic chlorinations.^{94,95} Equally, we propose that benzylic chlorinations in entries 6, 7, and 8 are a consequence of initial Cl^+ -delivery to the aromatic ring by **B** similar to the benzylic chlorination mechanism proposed Baciocchi and Illuminati for highly methylated arenes.⁹⁶ For example, in the reaction of $7 \cdot \text{Cl}^-$ with durene, the initially formed intermediate **B** would electrophilically deliver Cl^+ to the α - and the β -positions of the π -system to form **F** and **G** (Scheme 6). While **F** then produces the ring chlorination product, **G** undergoes a Baciocchi–Illuminati sequence including deprotonation and 1,5-Cl-shift from **H** to form the benzylic chlorination product. The observed biases for aromatic over benzylic chlorination products in entry 7 (aromatic/benzylic = 3.5:1) and entry 8 (aromatic/benzylic = 12:1) compare reasonably well with those found in previously reported electrophilic chlorinations of durene (aromatic/benzylic = 5.9:1)⁹⁷ and mesitylene with quantitative aromatic substitution.⁹⁸

Kinetic support for the intermediacy of **B** in the reaction of $7 \cdot \text{Cl}^-$ with hexamethylbenzene (HMB) is next discussed. At $[\text{HMB}] = 38.9 \text{ mM}$ ($\text{CDCl}_3/150 \text{ mM Bu}_4\text{NCl}$), the observed rate constant for benzylic chlorination was $k_{\text{obs}} = 22.2 \times 10^{-5} \text{ s}^{-1}$ (Table 3); this value is essentially identical to the previously determined $k_1^{\text{B}} = 20.1 \times 10^{-5} \text{ s}^{-1}$ and is consistent with the rate-determining formation of **B** in this reaction.

With less reactive aromatic substrates, the slow step in our model may not be the unimolecular formation of **B** anymore but instead the subsequent bimolecular Cl^+ -transfer from **B** to the π -system (for example, in the formation of **F** and **G** in Scheme 6). Indeed, the reactions of $7 \cdot \text{Cl}^-$ with the substrates 4-methylanisole ($k_{\text{bi}} = 2.1 \times 10^{-3} \text{ M}^{-1} \text{ s}^{-1}$) and 1,4-dimethoxybenzene ($k_{\text{bi}} = 6.1 \times 10^{-3} \text{ M}^{-1} \text{ s}^{-1}$) follow a bimolecular rate law: $d[7 \cdot \text{Cl}^-]/dt = k_1^{\text{B}}[7 \cdot \text{Cl}^-][\text{substrate}]$.

Even though our data on aromatic/benzylic chlorination are consistent with a ligand-mediated Cl^+ transfer from in situ generated **B**, we cannot definitively rule out metal-mediated processes including formation of $\text{Pd}^{\text{IV}}\text{-Ar}$ or $\text{Pd}^{\text{IV}}\text{-CH}_2\text{Ar}$ bonds. Such organometallic intermediates are commonly formed in Pd^{II} -based aromatic C–H bond activations via electrophilic aromatic substitutions,⁹⁹ concerted metalation–deprotonation,¹⁰⁰ or palladation/ β -elimination (Heck-like).¹⁰¹ Moreover, Sanford was able to form $\text{Pd}^{\text{IV}}\text{-Ar}$ bonds from proposed $[\text{Pd}^{\text{IV}}\text{-O}_2\text{CR}]$ intermediates.¹⁰² However, we consider a facile formation of

Scheme 6



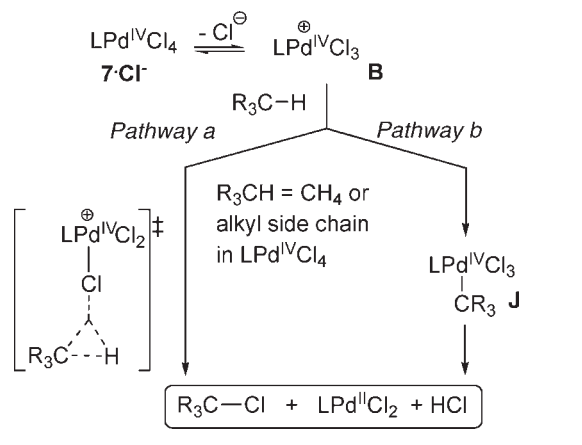
organometallic $\text{Pd}^{\text{IV}}\text{-C}_{\text{quart}}$ intermediates from 4-methylanisole and $7 \cdot \text{Cl}^-$ (entry 11, Table 1) to explain the preferred formation of 4-chloro-4-methylcyclohexa-2,5-dienone over 2-chloroanisole as rather implausible.

C–H bond activations by Pd^{IV} species were considered for the first time in 1971 in $\text{Pd}(\text{OAc})_2$ -catalyzed aromatic acetoxylation,^{11d} and recent sporadic reports have provided indirect experimental evidence that in situ generated Pd^{IV} species may indeed be capable of activating C–H bonds and form $\text{Pd}^{\text{IV}}\text{-Ar}$ bonds with¹⁰² or without chelation-control.¹⁰³ In contrast to these reports, our findings suggest that $\text{LPd}^{\text{IV}}\text{Cl}_4$ complex $7 \cdot \text{Cl}^-$ functionalizes aromatic and benzylic C–H bonds without the intermediate formation of $\text{Pd}^{\text{IV}}\text{-C}$ bonds. Product selectivities and kinetic evidence lend to the view that intermediate **B** is the reactive species in directly transferring Cl^+ to the aromatic π -system akin to Cl^+ -transfers from **B** to alkenes/alkynes.

Thermal Decomposition of $7 \cdot \text{Cl}^-$ via Side-Chain Chlorination and Chlorination of Methane. In the absence of suitable substrates, Pd^{IV} complex $7 \cdot \text{Cl}^-$ gradually decomposes in solution to Pd^{II} . Following this process by ^1H NMR spectroscopy revealed that the reduction of the metal center is accompanied by C–H chlorinations of the $\text{C}_{14}\text{H}_{29}$ side chain.¹⁰⁴ This process can be deliberately repeated in a catalytic fashion by reoxidizing the newly formed $\text{L}'\text{Pd}^{\text{II}}\text{Cl}_2$ complex in the presence of excess Cl_2 to $\text{L}'\text{Pd}^{\text{IV}}\text{Cl}_4$ ($\text{L}' = \text{bis-NHC ligand with a monochlorinated side chain}$).¹⁰⁵ In the presence of 1 atm Cl_2 (25 °C/16 h/ $\text{CDCl}_3/\text{Bu}_4\text{NCl}$), up to six side-chain chlorination events were recorded by ESI–MS.

The relevance of Pd^{IV} complexes in this chlorination process (rather than Cl_2 acting as the active aliphatic chlorinating agent) was established in a negative control experiment in which hexane (as a metal-free side-chain model) failed to produce chlorohexanes in the presence of 1 atm Cl_2 under otherwise identical reaction conditions. In an attempt to utilize this ability of $\text{LPd}^{\text{IV}}\text{Cl}_4$ to functionalize aliphatic C–H bonds, we probed for the complex's intermolecular ability to functionalize methane. Indeed, we identified the formation of CH_3Cl when a sample of CH_4 (1 atm in $\text{CDCl}_3/\text{Bu}_4\text{NCl}$) and $7 \cdot \text{Cl}^-$ were heated to 100 °C for 2 h in a sealed NMR tube. The extremely low yield in methyl chloride of 2.9% was a consequence of competing side-chain chlorination to ($\text{LPd}^{\text{IV}}\text{Cl}_4 \rightarrow \text{L}'\text{Pd}^{\text{II}}\text{Cl}_2$), while yields on

Scheme 7



the intermolecular functionalization may have also suffered from the relatively low pressure of methane in the experimental setup.

Recalling the *modus operandi* of chlorinations of π -systems by $7 \cdot \text{Cl}^-$, the chlorination of aliphatic C–H bonds is likely to involve the in situ generation of B (pathway a, Scheme 7). The latter may then insert Cl^+ into a C–H bond of methane or a side-chain C–H bond in $7 \cdot \text{Cl}^-$ via an electrophilic aliphatic substitution.¹⁰⁶ Such a reaction is reminiscent of electrophilic aliphatic methane chlorinations with Cl_2/SbF_5 ,¹⁰⁷ $\text{Cl}_2/\text{sulfated zirconia}$,¹⁰⁸ and of electrophilic alkane fluorination by F_2 .¹⁰⁹ Alternatively, we also considered an aliphatic C–H bond activation/functionalization involving $\text{Pd}^{\text{IV}}-\text{C}$ bonds in intermediate J (pathway b, Scheme 7) because Pd^{II} -, Pt^{II} -,^{16b,110} or rare Pt^{IV} -¹¹¹ mediated aliphatic C–H bond activations generally involve the intermediacy of organometallic complexes; aliphatic C–H bond activations by Pd^{IV} are unknown. Some indirect support for the general viability of complexes containing $\text{Pd}^{\text{IV}}-\text{C}$ bonds was found in the reaction of 7 with CH_3MgCl , which produced a 1:1 mixture of CH_3Cl and CH_3CH_3 and $\text{LPd}^{\text{II}}\text{Cl}_2$ (6) (entry 13, Table 1). The formation of ethane is indicative of a $\text{Pd}^{\text{IV}}-\text{dimethyl}$ intermediate $\text{LPd}^{\text{IV}}\text{Cl}_2(\text{CH}_3)_2$ that subsequently reductively eliminates CH_3CH_3 ; unlike their Pd^{II} -analogues, dialkyl Pd^{IV} species are susceptible to undergo C–C reductive elimination.^{2d} However, while CH_3Cl may have therefore been formed from $\text{LPd}^{\text{IV}}\text{Cl}_3(\text{CH}_3)$ in entry 13, this does not necessitate the formation of intermediate J in Scheme 7.

SUMMARY

Bis-NHC– Pd^{IV} -tetrachlorides ($\text{LPd}^{\text{IV}}\text{Cl}_4$) were isolated for the first time and employed as a chlorinating agent and oxidant for a variety of organic substrates, thus manifesting the feasibility of direct Pd^{IV} -functionalizations. Although stoichiometric in nature, this chemistry departs from the $\text{Pd}^{\text{II}}/\text{Pd}^{\text{IV}}$ paradigm (Scheme 1) that requires an initial activation of a substrate by Pd^{II} . Furthermore, under ambient conditions, $\text{LPd}^{\text{IV}}\text{Cl}_4$ was able to intermolecularly functionalize a variety of simple organic substrates without the need for a chelation process. Mechanistic studies on cyclohexene chlorinations elucidated a stepwise process involving cationic intermediates $\text{LPd}^{\text{IV}}\text{Cl}_3^+$ as active chlorinating agents; Cl^+ -transfers occurred via ligand-mediated routes.

We were able to chlorinate aromatic and benzylic C–H bonds of electron-rich aromatic systems with $\text{LPd}^{\text{IV}}\text{Cl}_4$. These reactions

proceed via chloroarenium ion intermediates. Methane was converted into methyl chloride in small yields. Through the establishment of $\text{C}-\text{H} \cdots \text{Cl}^-$ hydrogen bonds in the ligand periphery, we were able to modulate chemical reactivities of $\text{LPd}^{\text{IV}}\text{Cl}_4$ in alkene functionalizations. This supramolecular contact accelerated both Cl^- -dissociation from $\text{LPd}^{\text{IV}}\text{Cl}_4$ and Cl^+ -transfer from $\text{LPd}^{\text{IV}}\text{Cl}_3^+$. We propose that our results pave the way for direct activations of organic compounds via Pd^{IV} chemistry in future catalytic applications.

ASSOCIATED CONTENT

S Supporting Information. Detailed experimental procedures, spectroscopic characterizations, crystallographic data of compound 4, derivations of kinetic equations, and modeling of kinetic data. This material is available free of charge via the Internet at <http://pubs.acs.org>.

AUTHOR INFORMATION

Corresponding Author

skraft@ksu.edu

ACKNOWLEDGMENT

Financial support from NIH/K-INBRE (P 20 RR16475)-(SM), the Terry C. Johnson Cancer Center, the Kansas Lipidomics Research Center Analytical Laboratory (EPS 0236913, DBI 0521587), and Kansas State University is gratefully acknowledged. We thank G. W. Conrad for his support and guidance and D. R. M. Townsend, M. K. Higgins, A. L. May, and Y. Y. Yip for helpful discussions.

REFERENCES

- (1) Tsuji, J. *Palladium Reagents and Catalysts: New Perspectives for the 21st Century*, 2nd ed.; John Wiley & Sons Ltd.: Chichester, 2004.
- (2) (a) Xu, L. M.; Li, B. J.; Yang, Z.; Shi, Z. J. *Chem. Soc. Rev.* **2010**, *39*, 712–733. (b) Sehnal, P.; Taylor, R. J. K.; Fairlamb, I. J. S. *Chem. Rev.* **2010**, *110*, 824–889. (c) Sanford, M.; Lyons, T. W. *Chem. Rev.* **2010**, *110*, 1147–1169. (d) Canty, A. J. *J. Chem. Soc., Dalton Trans.* **2009**, 10409–10417. (e) Chen, X.; Engle, K. M.; Wang, D. H.; Yu, J. Q. *Angew. Chem., Int. Ed.* **2009**, *48*, 5094–5115.
- (3) (a) Canty, A. J. *Acc. Chem. Res.* **1992**, *25*, 83–90. (b) Alsters, P. L.; Engel, P. F.; Hogerheide, M. P.; Copijn, M.; Spek, A. L.; van Koten, G. *Organometallics* **1993**, *12*, 1831–1844. (c) Dick, A. R.; Kampf, J. W.; Sanford, M. S. *J. Am. Chem. Soc.* **2005**, *127*, 12790–12791. (d) Furuya, T.; Ritter, T. *J. Am. Chem. Soc.* **2008**, *130*, 10060–10061.
- (4) The first isolable organometallic Pd^{IV} compound was synthesized in 1975: Uson, R.; Fornies, J.; Navarro, R. J. *Organomet. Chem.* **1975**, *96*, 307–312.
- (5) (a) Byers, P. K.; Canty, A. J.; Crespo, M.; Puddephatt, R. J.; Scott, J. D. *Organometallics* **1988**, *7*, 1363–1367. (b) Canty, A. J.; Denney, M. C.; Skelton, B. W.; White, A. H. *Organometallics* **2004**, *23*, 1122–1131. (c) Canty, A. J.; Done, M. C.; Skelton, B. W.; White, A. H. *Inorg. Chem. Commun.* **2001**, *4*, 648–650. (d) Canty, A. J.; Hoare, J. L.; Davies, N. W.; Traill, P. R. *Organometallics* **1998**, *17*, 2046–2051. (e) Vanasselt, R.; Rijnberg, E.; Elsevier, C. J. *Organometallics* **1994**, *13*, 706–720. (f) Markies, B. A.; Canty, A. J.; Boersma, J.; van Koten, G. *Organometallics* **1994**, *13*, 2053–2058. (g) Markies, B. A.; Canty, A. J.; Janssen, M. D.; Spek, A. L.; Boersma, J.; van Koten, G. *Recl. Trav. Chim. Pays-Bas* **1991**, *110*, 477–479. (h) Byers, P. K.; Canty, A. J.; Traill, P. R.; Watson, A. A. *J. Organomet. Chem.* **1990**, *390*, 399–407. (i) Brown, D. G.; Byers, P. K.; Canty, A. J. *Organometallics* **1990**, *9*, 1231–1235. (j) Canty, A. J.; Watson, A. A.; Skelton, B. W.; White, A. H. *J. Organomet. Chem.* **1989**, *367*, C25–C28. (k) Byers, P. K.; Canty, A. J. *Chem. Commun.* **1988**,

- 639–641. (l) Byers, P. K.; Canty, A. J.; Skelton, B. W.; White, A. H. *Chem. Commun.* **1986**, 1722–1724.
- (6) (a) Racowski, J. M.; Dick, A. R.; Sanford, M. S. *J. Am. Chem. Soc.* **2009**, *131*, 10974–10983. (b) Dick, A. R.; Hull, K. L.; Sanford, M. S. *J. Am. Chem. Soc.* **2004**, *126*, 2300–2301.
- (7) Kruis, D.; Markies, B. A.; Canty, A. J.; Boersma, J.; van Koten, G. *J. Organomet. Chem.* **1997**, *532*, 235–242.
- (8) Aye, K. T.; Canty, A. J.; Crespo, M.; Puddephatt, R. J.; Scott, J. D.; Watson, A. A. *Organometallics* **1989**, *8*, 1518–1522.
- (9) (a) Daugulis, O.; Zaitsev, V. G. *Angew. Chem., Int. Ed.* **2005**, *44*, 4046–4048. (b) McCallum, J. S.; Gasdaska, J. R.; Liebeskind, L. S.; Tremont, S. J. *Tetrahedron Lett.* **1989**, *30*, 4085–4088. (c) Tremont, S. J.; Rahman, H. U. *J. Am. Chem. Soc.* **1984**, *106*, 5759–5760. (d) Zaitsev, V. G.; Shabashov, D.; Daugulis, O. *J. Am. Chem. Soc.* **2005**, *127*, 13154–13155.
- (10) As stated in ref 2b: “One ultimate challenge facing the Pd^{IV} field is to selectively activate sp³ C–H and C–C bonds, without the need for proximal directing groups (e.g., imino or amino substituents).”
- (11) (a) Yoneyama, T.; Crabtree, R. H. *J. Mol. Catal. A: Chem.* **1996**, *108*, 35–40. (b) Jintoku, T.; Taniguchi, H.; Fujiwara, Y. *Chem. Lett.* **1987**, 1865–1868. (c) Stock, L. M.; Tse, K.; Vorvick, L. J.; Walstrum, S. A. *J. Org. Chem.* **1981**, *46*, 1757–1759. (d) Henry, P. M. *J. Org. Chem.* **1971**, *36*, 1886–1890.
- (12) (a) Diez-Gonzalez, S.; Marion, N.; Nolan, S. P. *Chem. Rev.* **2009**, *109*, 3612–3676. (b) de Fremont, P.; Marion, N.; Nolan, S. P. *Coord. Chem. Rev.* **2009**, *253*, 862–892. (c) Normand, A. T.; Cavell, K. J. *Eur. J. Inorg. Chem.* **2008**, 2781–2800. (d) Diez-Gonzalez, S.; Nolan, S. P. *Coord. Chem. Rev.* **2007**, *251*, 874–883. (e) Herrmann, W. A.; Schutz, J.; Frey, G. D.; Herdtweck, E. *Organometallics* **2006**, *25*, 2437–2448. (f) Crudden, C. M.; Allen, D. P. *Coord. Chem. Rev.* **2004**, *248*, 2247–2273. (g) Herrmann, W. A. *Angew. Chem., Int. Ed.* **2002**, *41*, 1290–1309. (h) Herrmann, W. A.; Weskamp, T.; Bohm, V. P. W. *Adv. Organomet. Chem.* **2001**, *48*, 1–69. (i) Herrmann, W. A.; Kocher, C. *Angew. Chem., Int. Ed. Engl.* **1997**, *36*, 2162–2187.
- (13) Jain, K. R.; Herrmann, W. A.; Kuhn, F. E. *Curr. Org. Chem.* **2008**, *12*, 1468–1478.
- (14) Arnold, P. L.; Sanford, M. S.; Pearson, S. M. *J. Am. Chem. Soc.* **2009**, *131*, 13912–13913.
- (15) (a) Kuhl, O. *Coord. Chem. Rev.* **2009**, *253*, 2481–2492. (b) Cavell, K. J. *Chem. Soc., Dalton Trans.* **2008**, 6676–6685. (c) Graham, D. C.; Cavell, K. J.; Yates, B. F. *J. Chem. Soc., Dalton Trans.* **2005**, 1093–1100. (d) Clement, N. D.; Cavell, K. J. *Angew. Chem., Int. Ed.* **2004**, *43*, 3845–3847. (e) Cavell, K. J.; McGuinness, D. S. *Coord. Chem. Rev.* **2004**, *248*, 671–681. (f) McGuinness, D. S.; Saendig, N.; Yates, B. F.; Cavell, K. J. *J. Am. Chem. Soc.* **2001**, *123*, 4029–4040.
- (16) (a) Muehlhofer, M.; Strassner, T.; Herrmann, W. A. *Angew. Chem., Int. Ed.* **2002**, *41*, 1745–1747. (b) Strassner, T.; Muehlhofer, M.; Zeller, A.; Herdtweck, E.; Herrmann, W. A. *J. Organomet. Chem.* **2004**, *689*, 1418–1424.
- (17) Gray, L. R.; Gulliver, D. J.; Levason, W.; Webster, M. J. *Chem. Soc., Dalton Trans.* **1983**, 133–141.
- (18) Babaeva, A. V.; Khananova, E. Y. *Dokl. Akad. Nauk SSSR* **1964**, *159*, 586–7.
- (19) (a) Kalyani, D.; Dick, A. R.; Anani, W. Q.; Sanford, M. S. *Org. Lett.* **2006**, *8*, 2523–2526. (b) Kalyani, D.; Dick, A. R.; Anani, W. Q.; Sanford, M. S. *Tetrahedron* **2006**, *62*, 11483–11498. (c) Whitfield, S. R.; Sanford, M. S. *J. Am. Chem. Soc.* **2007**, *129*, 15142–15143.
- (20) Arnold, P. L.; Zlatogorsky, S.; Jones, N. A.; Carmichael, C. D.; Liddle, S. T.; Blake, A. J.; Wilson, C. *Inorg. Chem.* **2008**, *47*, 9042–9049.
- (21) Less coordinating salts such as LiClO₄, LiOTf, or NaBPh₄ did not assist dissolving **7** in CDCl₃, CD₂Cl₂, or CDCl₂CDCl₂ in any appreciable fashion. This suggests that the establishment of a trifurcated hydrogen bond in **7**·Cl[−] is necessary to break up packing forces in the solid state of **7**. Similarly, BF₄[−] may be able to interact with **7** in a similar fashion, yet to a weaker extent than Cl[−]. The observation that at least 5 equiv of Bu₄NBF₄ is needed to dissolve 1 equiv of **7** while only 1 equiv of Bu₄NCl is required qualitatively agrees with this hypothesis. Anions with even poorer hydrogen-bonding capabilities such as ClO₄[−], TfO[−], or BPh₄[−] are apparently not able to disrupt the solid state network of **7**.
- (22) Bromination of LPd^{II}Br₂ (**2**) with Br₂ in neat TFA produced a yellow precipitate of putative LPd^{IV}Br₄. After the solvent was evaporated and dried for 1 h under high vacuum, the sample turned colorless again, and we regenerated **2** with an apparent loss of Br₂.
- (23) Attempts to produce related LPd^{IV}X₄ species from **1**, **2**, or **6** with O- or F-based oxidants [PhI(OAc)₂, PhI(OTFA)₂, *t*-BuOO-*t*-Bu, (PhCO₂)O (all in CDCl₃), K₂S₂O₈, KHSO₅, (both in TFA-*d*), and selectfluor (in CD₃CN)] caused no noticeable changes in the ¹H NMR spectrum of the respective Pd^{II} starting material. Reaction of **6** with XeF₂ produced complex mixtures. Treatment of **6** with AgF to form LPdF₂ in situ followed by addition of XeF₂ led to unidentifiable product mixtures as well.
- (24) (a) Hirose, K. *J. Inclusion Phenom. Macrocyclic Chem.* **2001**, *39*, 193–209. (b) Job, P. *Ann. Chim.* **1928**, *9*, 113. (c) Job, P. *Comptes Rendus* **1925**, *180*, 928–930.
- (25) Remsing, R. C.; Swatloski, R. P.; Rogers, R. D.; Moyna, G. *Chem. Commun.* **2006**, 1271–1273.
- (26) (a) Uemura, S.; Sasaki, O.; Okano, M. *Bull. Chem. Soc. Jpn.* **1972**, *45*, 1482–1484. (b) Onoe, A.; Uemura, S.; Okano, M. *Bull. Chem. Soc. Jpn.* **1976**, *49*, 345–346.
- (27) Henniger, P. W.; Dukker, L. J.; Havinga, E. *Recl. Trav. Chim. Pays-Bas* **1966**, *85*, 1177–1187.
- (28) Timokhin, B. V. *Usp. Khim.* **1985**, *54*, 2027–2043.
- (29) Heasley, V. L.; Rold, K. D.; Titterington, D. R.; Leach, C. T.; Gipe, B. T.; McKee, D. B.; Heasley, G. E. *J. Org. Chem.* **1976**, *41*, 3997–4001.
- (30) Nugent, W. A. *J. Org. Chem.* **1980**, *45*, 4533–4534.
- (31) Chung, S. K. *Tetrahedron Lett.* **1978**, 3211–3214.
- (32) Tanner, D. D.; Gidley, G. C. *J. Org. Chem.* **1968**, *33*, 38–43.
- (33) Gulliver, D. J.; Levason, W. *Coord. Chem. Rev.* **1982**, *46*, 1–127.
- (34) Kukushkin, Y. N.; Sedova, G. N.; Vlasova, R. A. *Zh. Neorg. Khim.* **1978**, *23*, 1877–83.
- (35) Babaeva, A. V.; Khananova, E. Y. *Zh. Neorg. Khim.* **1965**, *10*, 2579–81.
- (36) Gulliver, D. J.; Levason, W. J. *Chem. Soc., Dalton Trans.* **1982**, 1895–1898.
- (37) In a concerted loss of Cl₂, two Pd–Cl bonds would break at the same time concomitant with a change of the oxidation state of the metal from +4 to +2. In contrast, a stepwise route would entail an initial dissociation of Cl[−] followed by a Cl⁺ transfer from LnPd^{IV}Cl₃⁺ to Cl[−] to form Cl₂. The metal is reduced in the second step. This ionic sequence is reminiscent of pathway 3b (Scheme 4).
- (38) Furuya, T.; Benitez, D.; Tkatchouk, E.; Strom, A. E.; Tang, P.; Goddard, W. A.; Ritter, T. *J. Am. Chem. Soc.* **2010**, *132*, 3793–3807.
- (39) (a) Jensen, M. P.; Wick, D. D.; Reinartz, S.; White, P. S.; Templeton, J. L.; Goldberg, K. I. *J. Am. Chem. Soc.* **2003**, *125*, 8614–8624. (b) Crumpton-Bregel, D. M.; Goldberg, K. I. *J. Am. Chem. Soc.* **2003**, *125*, 9442–9456. (c) Williams, B. S.; Goldberg, K. I. *J. Am. Chem. Soc.* **2001**, *123*, 2576–2587.
- (40) Uemura, S.; Onoe, A.; Okano, M. *Bull. Chem. Soc. Jpn.* **1974**, *47*, 692–697.
- (41) Gamlen, P. H.; Henty, M. S.; Roberts, H. L. *J. Chem. Soc., Dalton Trans.* **1983**, 1373–1376.
- (42) Sundermann, A.; Uzan, O.; Martin, J. M. L. *Chem.-Eur. J.* **2001**, *7*, 1703–1711.
- (43) (a) Bäckvall, J. E.; Nilsson, Y. I. M.; Gatti, R. G. P. *Organometallics* **1995**, *14*, 4242–4246. (b) Bäckvall, J. E.; Nilsson, Y. I. M.; Andersson, P. G.; Gatti, R. G. P.; Wu, J. C. *Tetrahedron Lett.* **1994**, *35*, 5713–5716. (c) Wipke, W. T.; Goeke, G. L. *J. Am. Chem. Soc.* **1974**, *96*, 4244–4249.
- (44) Poutsma, M. L. *J. Am. Chem. Soc.* **1965**, *87*, 4285–4293.
- (45) Collman, J. P.; Hegedus, L. S.; Norton, J. R.; Finke, R. G. *Principles and Applications of Organotransition Metal Chemistry*; University Science Books: Mill Valley, CA, 1987; p 149.
- (46) (a) Cavell, K. J. *Coord. Chem. Rev.* **1996**, *155*, 209–243. (b) Tye, J. W.; Hartwig, J. F. *J. Am. Chem. Soc.* **2009**, *131*, 14703–14712. (c) Gürtler, C.; Buchwald, S. L. *Chem.-Eur. J.* **1999**, *5*, 3107–3112. (d) Heck, R. F. *Acc. Chem. Res.* **1979**, *12*, 146–151. (e) Larock, R. C.;

Takagi, K. *J. Org. Chem.* **1984**, *49*, 2701–2705. (f) Larock, R. C.; Fried, C. A. *J. Am. Chem. Soc.* **1990**, *112*, 5882–5884. (g) Albeniz, A. C.; Espinet, P.; Lin, Y. S. *Organometallics* **1995**, *14*, 2977–2986. (h) Stakem, F. G.; Heck, R. F. *J. Org. Chem.* **1980**, *45*, 3584–3593. (i) Mabbott, D. J.; Maitlis, P. M. *J. Chem. Soc., Dalton Trans.* **1976**, 2156–2160. (j) Liu, G. S.; Stahl, S. S. *J. Am. Chem. Soc.* **2006**, *128*, 7179–7181. (k) Brice, J. L.; Harang, J. E.; Timokhin, V. I.; Anastasi, N. R.; Stahl, S. S. *J. Am. Chem. Soc.* **2005**, *127*, 2868–2869. (l) Paiaro, G.; Derenzi, A.; Palumbo, R. *Chem. Commun.* **1967**, 1150–1151. (m) Bäckvall, J. E. *Acc. Chem. Res.* **1983**, *16*, 335–342. (n) Bäckvall, J. E.; Nordberg, R. E.; Nystrom, J. E. *Tetrahedron Lett.* **1982**, *23*, 1617–1620.

(47) We omitted data from entry 1 (Table 3) in Figure 3 for visual clarity regarding early data points. However, k_{obs} values are identical in entries 1 and 2, which underlines the validity of a [cy]-independent k_{obs} plateau.

(48) We corrected k_{obs} data from entries 21–24 by subtracting rate contributions of small amounts of $7 \cdot \text{Cl}^-$ ($\chi_{7 \cdot \text{Cl}^-} = 0.080-0.045$) in the system. These corrections amounted to less than $1.6 \times 10^{-5} \text{ s}^{-1}$ and did not affect the conclusion that $7 \cdot \text{Cl}^-$ is noticeably more reactive than 7.

(49) In the presence of chloride ions, chemical shifts of 7 and $7 \cdot \text{Cl}^-$ are indistinguishable on the NMR time scale, and their equilibration ($7 + \text{Cl}^-_{\text{free}} \rightleftharpoons 7 \cdot \text{Cl}^-$) is therefore faster than substrate chlorinations ($t_{1/2}$ of 1 h).

(50) An alternative explanation for the bias against the formation of B in entries 21–24 (Table 3) may be sought by assuming that the structure of intermediate A is that of the free cation $\text{LPd}^{\text{IV}}\text{Cl}_3^+$ devoid of any localized interactions within a tight ion pair with Cl^- or BF_4^- . A hypothetical equilibrium $\text{B} \rightleftharpoons \text{LPd}^{\text{IV}}\text{Cl}_3^+ + \text{Cl}^-_{\text{free}}$ with $K_{\text{eq}}(\text{B}) = [\text{LPd}^{\text{IV}}\text{Cl}_3^+][\text{Cl}^-_{\text{free}}]/[\text{B}]$ would then favor the formation of $\text{LPd}^{\text{IV}}\text{Cl}_3^+$ at the expense of B at low $[\text{Cl}^-_{\text{free}}]$. A reasonable lower estimate for the ion pair association constant $K_{\text{eq}}(\text{B})$ in the non-polar solvent CDCl_3 (that only includes electrostatic attractions but no specific hydrogen-bonding effects) would be $\geq 100,000 \text{ M}^{-1}$ based on $\text{Bu}_4\text{N}^+\text{ClO}_4^-$ association constants in solvents with $\epsilon \leq 10$ (Janz, C. G.; Tomkins, R. P. T. *Non-Aqueous Electrolytes Handbook*; Academic Press: New York, 1972). Using the lowest free chloride concentration in our experiments $[\text{Cl}^-_{\text{free}}] = 0.00034 \text{ M}$ (entry 23, Table 3) as well as $K_{\text{eq}}(\text{B}) \geq 100,000 \text{ M}^{-1}$ in $[\text{B}]/[\text{LPd}^{\text{IV}}\text{Cl}_3^+] = 1/(K_{\text{eq}}(\text{B})[\text{Cl}^-_{\text{free}}])$ (derived from the equilibrium equation above) yields the ratio $[\text{B}]/[\text{LPd}^{\text{IV}}\text{Cl}_3^+] \geq 34$. On the basis of the conservative estimate for the value of $K_{\text{eq}}(\text{B})$, even our experimentally lowest value of $[\text{Cl}^-_{\text{free}}]$ would therefore not be low enough to produce significant quantities of free $[\text{LPd}^{\text{IV}}\text{Cl}_3^+]$ at the expense of B. Therefore, this thermodynamic argument is an unlikely explanation for the bias against the formation of B in entries 21–24. We therefore favor a kinetic interpretation of an inhibited formation of B on the timescale of k_{-1} and k_2 from an intermediate A that is best described as hydrogen-bonded adduct $\text{BF}_4^- \cdots \text{LPd}^{\text{IV}}\text{Cl}_3^+$.

(51) cks was developed by IBM-Almaden Lab and can be downloaded free of charge from http://www.almaden.ibm.com/st/computational_science/ck/.

(52) (a) Bunker, D. L.; Garrett, B.; Kleindienst, T.; Long, G. S. *Combust. Flame* **1974**, *23*, 373–379. (b) Gillespie, D. T. *J. Comput. Phys.* **1976**, *22*, 403–434.

(53) Without the ability to measure in situ concentrations of A and B, absolute values of k_{-1}^A , k_{-1}^B , k_2^A , and k_2^B could not be determined.

(54) The upper value of $\Delta G(\text{exchange}) = 14.0 \text{ kcal mol}^{-1}$ for the exchange process $7 \cdot \text{Cl}^- \rightleftharpoons 7 + \text{Cl}^-_{\text{free}} \rightleftharpoons 7 \cdot \text{Cl}^-$ was determined from $\Delta\nu = 148 \text{ Hz}$ from frequencies associated with proton H^5 in discreet samples of pure 7 as well as $7 \cdot \text{Cl}^-$ [operating frequency: 400 MHz; $k(\text{exchange}) \geq 2.22 (\Delta\nu)$].

(55) The choice of recruiting different Pd^{IV} -tetrachlorides in the two solvents was due to limited solubility characteristics of $\text{LPd}^{\text{IV}}\text{Cl}_4$ species; ditetradecyl-substituted complex 7 could only be dissolved in chlorinated solvents in the presence of electrolytes; 7 was virtually insoluble in other common organic solvents (with or without adding Bu_4NCl) such as hexane, diethylether, benzene, THF, ethyl acetate, acetone, acetonitrile, DMF, and methanol. Similar limitations were encountered with dimethyl-substituted 4 that showed measurable solubility exclusively in DMF.

(56) We gratefully acknowledge an alternative explanation by a reviewer who pointed out the “possibility that the relatively long $\text{NHC-Pd}^{\text{IV}}$ distance might reflect the poor overlap between the soft carbene carbon and the much hardened Pd^{IV} center.”

(57) (a) Khramov, D. M.; Lynch, V. M.; Bielawski, C. W. *Organometallics* **2007**, *26*, 6042–6049. (b) Fantasia, S.; Petersen, J. L.; Jacobsen, H.; Cavallo, L.; Nolan, S. P. *Organometallics* **2007**, *26*, 5880–5889. (c) Jacobsen, H.; Correa, A.; Costabile, C.; Cavallo, L. *J. Organomet. Chem.* **2006**, *691*, 4350–4358. (d) Scott, N. M.; Nolan, S. P. *Eur. J. Inorg. Chem.* **2005**, 1815–1828.

(58) Baba, E.; Cundari, T. R.; Firkin, I. *Inorg. Chim. Acta* **2005**, *358*, 2867–2875.

(59) (a) Appleton, T. G.; Clark, H. C.; Manzer, L. E. *Coord. Chem. Rev.* **1973**, *10*, 335–422. (b) Pidcock, A.; Richards, R. E.; Venanzi, L. M. *J. Chem. Soc. A* **1966**, 1707–1710.

(60) Baker, M. V.; Brown, D. H.; Heath, C. H.; Skelton, B. W.; White, A. H.; Williams, C. C. *J. Org. Chem.* **2008**, *73*, 9340–9352.

(61) Li, Y. L.; Flood, A. H. *J. Am. Chem. Soc.* **2008**, *130*, 12111–12122.

(62) (a) Fortin, S.; Beauchamp, A. L. *Inorg. Chem.* **2001**, *40*, 105–112. (b) Fortin, S.; Fabre, P. L.; Dartiguenave, M.; Beauchamp, A. L. *J. Chem. Soc., Dalton Trans.* **2001**, 3520–3527.

(63) (a) Böttcher, L.; Scholz, A.; Walther, D.; Weisbach, N.; Görls, H. Z. *Anorg. Allg. Chem.* **2003**, *629*, 2103–2112. (b) Rau, S.; Böttcher, L.; Schebesta, S.; Stollenz, M.; Görls, H.; Walther, D. *Eur. J. Inorg. Chem.* **2002**, 2800–2809.

(64) Romeo, R.; Nastasi, N.; Scolaro, L. M.; Plutino, M. R.; Albinati, S.; Macchioni, A. *Inorg. Chem.* **1998**, *37*, 5460–5466.

(65) Appelhans, L. N.; Zuccaccia, D.; Kovacevic, A.; Chianese, A. R.; Miecznikowski, J. R.; Macchioni, A.; Clot, E.; Eisenstein, O.; Crabtree, R. H. *J. Am. Chem. Soc.* **2005**, *127*, 16299–16311.

(66) Herrmann, W. A.; Öfele, K.; Von Preysing, D.; Schneider, S. K. *J. Organomet. Chem.* **2003**, *687*, 229–248.

(67) Wong, P. K.; Stille, J. K. *J. Organomet. Chem.* **1974**, *70*, 121–132.

(68) Pilarski, L. T.; Selander, N.; Böse, D.; Szabo, K. *J. Org. Lett.* **2009**, *11*, 5518–5521.

(69) Trost, B. M.; Lautens, M. *Tetrahedron Lett.* **1985**, *26*, 4887–4890.

(70) In nonpolar solvents, quarternary ammonium salts are not dissociated to any appreciable degree with dissociation enthalpies of 24.3 kcal mol⁻¹ for tetra-*i*-amylammonium chloride in benzene [Fuoss, R. M.; Kraus, C. A. *J. Am. Chem. Soc.* **1933**, *55*, 3614–3620] or 6.3 kcal mol⁻¹ for tetrabutylammonium chloride in CH_2Cl_2 . (a) Balt, S.; Duchattel, G.; Dekieviet, W.; Tieleman, A. Z. *Naturforsch., B: J. Chem. Sci.* **1978**, *33*, 745–749. (b) Svorstol, I.; Hoiland, H.; Songstad, J. *Acta Chem. Scand., Ser. B* **1984**, *38*, 885–893].

(71) A direct solvent comparison for one exclusive species was not possible, as 7 was insoluble in DMF-*d*₇ and in other solvents with high dielectric constants, while compound 4 was only soluble in DMF-*d*₇ yet insoluble in other organic solvents. The addition of electrolytes such as Bu_4NCl or Bu_4NBF_4 did not rectify these solubility problems.

(72) The dielectric constants of DMF-*d*₇ ($\sum = 36.7$) and CDCl_3 ($\sum = 4.8$) diverge greatly. However, the addition of electrolytes (10^{-2} – 10^{-1} M range) to unpolar solvents ($\sum < 12$) can increase the dielectric constant by 100% [(a) Cachet, H.; Cyrot, A.; Fekir, M.; Lestrade, J. C. *J. Phys. Chem.* **1979**, *83*, 2419–2429. (b) Cavell, E. A. S.; Knight, P. C. *J. Phys. Chem.* **1968**, *57*, 331–334. (c) Svorstol, I.; Hoiland, H.; Songstad, J. *Acta Chem. Scand., Ser. B* **1984**, *38*, 885–893].

(73) (a) Nelson, D. J.; Li, R. B.; Brammer, C. J. *Phys. Org. Chem.* **2004**, *17*, 1033–1038. (b) Awasthy, A. K.; Rocek, J. *J. Am. Chem. Soc.* **1969**, *91*, 991–996.

(74) Sharpless, K. B.; Williams, D. R. *Tetrahedron Lett.* **1975**, 3045–3046.

(75) Nelson, D. J.; Li, R. B.; Brammer, C. J. *Org. Chem.* **2001**, *66*, 2422–2428.

(76) (a) Wang, A. Z.; Jiang, H. F.; Chen, H. J. *J. Am. Chem. Soc.* **2009**, *131*, 3846–3847. (b) Li, Y.; Song, D.; Dong, V. M. *J. Am. Chem. Soc.* **2008**, *130*, 2962–2964.

- (77) (a) Alexanian, E. J.; Lee, C.; Sorensen, E. J. *J. Am. Chem. Soc.* **2005**, *127*, 7690–7691. (b) Streuff, J.; Hövelmann, C. H.; Nieger, M.; Muniz, K. *J. Am. Chem. Soc.* **2005**, *127*, 14586–14587. (c) Desai, L. V.; Sanford, M. S. *Angew. Chem., Int. Ed.* **2007**, *46*, 5737–5740. (d) Muniz, K.; Hövelmann, C. H.; Streuff, J. *J. Am. Chem. Soc.* **2008**, *130*, 763–773.
- (78) Kalyani, D.; Sanford, M. S. *J. Am. Chem. Soc.* **2008**, *130*, 2150–2151.
- (79) We define the term “activation” as the step that establishes Pd–C σ -bonds from either an alkene or a C–H bond.
- (80) (a) Stang, P.; Zhdankin, V. *Chem. Rev.* **1996**, *96*, 1123–1178. (b) Zhdankin, V. V.; Stang, P. J. *Chem. Rev.* **2002**, *102*, 2523–2584. (c) Zhdankin, V. V.; Stang, P. J. *Chem. Rev.* **2008**, *108*, 5299–5358. (d) Deprez, N. R.; Sanford, M. S. *Inorg. Chem.* **2007**, *46*, 1924–1935. (e) Desai, L. V.; Hull, K. L.; Sanford, M. S. *J. Am. Chem. Soc.* **2004**, *126*, 9542–9543. (f) Hull, K. L.; Anani, W. Q.; Sanford, M. S. *J. Am. Chem. Soc.* **2006**, *128*, 7134–7135. (g) Furuya, T.; Kaiser, H. M.; Ritter, T. *Angew. Chem., Int. Ed.* **2008**, *47*, 5993–5996. (h) Wang, X. S.; Mei, T. S.; Yu, J. Q. *J. Am. Chem. Soc.* **2009**, *131*, 7520–7521.
- (81) (a) Smith, P. J.; Kim, E. L.; Wilcox, C. S. *Angew. Chem., Int. Ed. Engl.* **1993**, *32*, 1648–1650. (b) Smith, P. J.; Reddington, M. V.; Wilcox, C. S. *Tetrahedron Lett.* **1992**, *33*, 6085–6088. (c) Heuze, K.; Meziere, C.; Fourmigue, M.; Batail, P.; Coulon, C.; Canadell, E.; Auban-Senzier, P.; Jerome, D. *Chem. Mater.* **2000**, *12*, 1898–1904.
- (82) Winstein, S.; Clipping, E.; Fainberg, A. H.; Robinson, G. C. *J. Am. Chem. Soc.* **1954**, *76*, 2597–2598.
- (83) Typically, special salt effects play out in intercepting in situ formed ion pairs (intimate or solvent separated) through cation or anion exchange, thus altering the reactivity of the system, for example, by slowing internal return reactions. Rate accelerations are nonlinear, and k_{obs} reaches a plateau or a linear domain that itself is only affected only by the common salt effect (rate changes through increase in ion strength). See: Dvorko, G. F.; Ponomareva, E. A.; Ponomarev, N. E. *Russ. J. Gen. Chem.* **2006**, *76*, 1368–1385.
- (84) The definition of heteroconjugation is “the conjugation of an anion A^- with a hydrogen-bond donor”. See: Koltzoff, I. M.; Chantooni, M. K. *J. Am. Chem. Soc.* **1963**, *85*, 2195–2201.
- (85) An internal return reaction of **B** would require a rearrangement of peripherally bonded Cl^- to the metal center and would initially form **7**; subsequently, $7 \cdot \text{Cl}^-$ is rapidly formed in the presence of Bu_4NCl .
- (86) (a) Poulton, J. T.; Sigalas, M. P.; Folting, K.; Streib, W. E.; Eisenstein, O.; Caulton, K. G. *Inorg. Chem.* **1994**, *33*, 1476–1485. (b) Poulton, J. T.; Folting, K.; Streib, W. E.; Caulton, K. G. *Inorg. Chem.* **1992**, *31*, 3190–3191.
- (87) (a) Fuoss, R. M.; Kraus, C. A. *J. Am. Chem. Soc.* **1933**, *55*, 2387–2399. (b) Fuoss, R. M.; Kraus, C. A. *J. Am. Chem. Soc.* **1933**, *55*, 2387–2399. (c) Marcus, Y.; Hefter, G. *Chem. Rev.* **2006**, *106*, 4585–4621.
- (88) As our information on **A** is limited to kinetic data, we cannot exclude tight or solvent-separated ion pairs $\text{LPd}^{\text{IV}}\text{Cl}_3^+\text{BF}_4^-$ and $\text{LPd}^{\text{IV}}\text{Cl}_3^+(\text{solvent})\text{BF}_4^-$ from consideration for the structure of **A**.
- (89) Shannon, R. D. *Acta Crystallogr., Sect. A: Found. Crystallogr.* **1976**, *32*, 751–767.
- (90) Hofstetter, C.; Pochapsky, T. C. *Magn. Reson. Chem.* **2000**, *38*, 90–94.
- (91) Macchioni, A. *Chem. Rev.* **2005**, *105*, 2039–2073.
- (92) (a) Yabe, T.; Kochi, J. K. *J. Am. Chem. Soc.* **1992**, *114*, 4491–4500. (b) Simon, J. D.; Peters, K. S. *J. Am. Chem. Soc.* **1982**, *104*, 6542–6547.
- (93) (a) Fuoss, R. M.; Kraus, C. A. *J. Am. Chem. Soc.* **1935**, *57*, 1–4. (b) Winstein, S.; Klinedinst, P. E.; Robinson, G. C. *J. Am. Chem. Soc.* **1961**, *83*, 885–895. (c) Petrucci, S.; Masiker, M. C.; Eyring, E. M. *J. Solution Chem.* **2008**, *37*, 1031–1035.
- (94) Smith, J. R. L.; McKeer, L. C.; Taylor, J. M. *J. Chem. Soc., Perkin Trans. 2* **1989**, 1529–1536.
- (95) Smith, J. R. L.; McKeer, L. C.; Taylor, J. M. *J. Chem. Soc., Perkin Trans. 2* **1988**, 385–391.
- (96) (a) Baciocchi, E.; Illuminati, G. *Tetrahedron Lett.* **1962**, 637–641. (b) Baciocchi, E.; Ciana, A.; Illuminati, G.; Pasini, C. *J. Am. Chem. Soc.* **1965**, *87*, 3953–3957. (c) Illuminati, G.; Mandolini, L.; Baciocchi, E.; Patara, A. *Tetrahedron Lett.* **1972**, 4161–4164. (d) Baciocchi, E.; Illuminati, G. *Tetrahedron Lett.* **1975**, 2265–2267. (e) Baciocchi, E.; Mandolini, L. *Tetrahedron* **1987**, *43*, 4035–4041. (f) Baciocchi, E.; Galli, C. *J. Phys. Org. Chem.* **1995**, *8*, 563–565.
- (97) Andrews, L. J.; Keefer, R. M. *J. Am. Chem. Soc.* **1960**, *82*, 5823–5826.
- (98) Fittig, R.; Hoogewerff, S. *Liebigs Ann. Chem. Pharm.* **1869**, *150*, 323–338.
- (99) (a) Catellani, M.; Chiusoli, G. P. *J. Organomet. Chem.* **1992**, *425*, 151–154. (b) Martin-Matute, B.; Mateo, C.; Cardenas, D. J.; Echavaren, A. M. *Chem.-Eur. J.* **2001**, *7*, 2341–2348. (c) Park, C. H.; Ryabova, V.; Seregin, I. V.; Sromek, A. W.; Gevorgyan, V. *Org. Lett.* **2004**, *6*, 1159–1162. (d) Pivsa-Art, S.; Satoh, T.; Kawamura, Y.; Miura, M.; Nomura, M. *Bull. Chem. Soc. Jpn.* **1998**, *71*, 467–473. (e) Lane, B. S.; Brown, M. A.; Sames, D. *J. Am. Chem. Soc.* **2005**, *127*, 8050–8057. (f) Li, J. J.; Giri, R.; Yu, J. Q. *Tetrahedron* **2008**, *64*, 6979–6987.
- (100) (a) Gorelsky, S. I.; Lapointe, D.; Fagnou, K. *J. Am. Chem. Soc.* **2008**, *130*, 10848–10849. (b) Lafrance, M.; Fagnou, K. *J. Am. Chem. Soc.* **2006**, *128*, 16496–16497. (c) Lafrance, M.; Rowley, C. N.; Woo, T. K.; Fagnou, K. *J. Am. Chem. Soc.* **2006**, *128*, 8754–8756. (d) Garcia-Cuadrado, D.; de Mendoza, P.; Braga, A. A. C.; Maseras, F.; Echavaren, A. M. *J. Am. Chem. Soc.* **2007**, *129*, 6880–6886. (e) Garcia-Cuadrado, D.; Braga, A. A. C.; Maseras, F.; Echavarren, A. M. *J. Am. Chem. Soc.* **2006**, *128*, 1066–1067.
- (101) Glover, B.; Harvey, K. A.; Liu, B.; Sharp, M. J.; Tymoschenko, M. F. *Org. Lett.* **2003**, *5*, 301–304.
- (102) Hull, K.; Lanni, E.; Sanford, M. *J. Am. Chem. Soc.* **2006**, *128*, 14047–14049.
- (103) Rosewall, C.; Sibbald, P.; Liskin, D.; Michael, F. *J. Am. Chem. Soc.* **2009**, *131*, 9488–9489.
- (104) When $7 \cdot \text{Cl}^-$ was heated at 100 °C in CDCl_3 for 30 min, ^1H NMR signals associated with Pd^{IV} complex **7**· Cl^- completely disappeared. New multiplets consistent with side-chain chlorinations in the β -, γ -, and δ -site were found at δ 4.6–4.4, 4.2–4.0, and 3.75–3.65 integrating for 0.52 H, 0.35 H, and 0.10 H relative to the aromatic signals that are indicative of a pseudosymmetrical Pd^{II} scaffold (δ 7.85 (2H), 6.80 (2H)).
- (105) In contrast to Strassner’s proposed $\text{Pd}^{\text{II}}/\text{Pd}^{\text{IV}}$ catalysis [ref 16b] for methane activation with **1** and **2**, we suggest an “inverted” $\text{Pd}^{\text{IV}}/\text{Pd}^{\text{II}}$ sequence of events, in which the role of Pd^{II} is limited to the reaction with Cl_2 to regenerate Pd^{IV} , which may serve to expand the horizon of Strassner’s platform in the future.
- (106) Olah, G. A. *Acc. Chem. Res.* **1987**, *20*, 422–428.
- (107) Olah, G. A. *Pure Appl. Chem.* **1981**, *53*, 201–207.
- (108) Batamack, P.; Bucsi, I.; Molnar, A.; Olah, G. A. *Catal. Lett.* **1994**, *25*, 11–19.
- (109) (a) Rozen, S. *Acc. Chem. Res.* **1988**, *21*, 307–312. (b) Chambers, R. D.; Parsons, M.; Sandford, G.; Thomas, E.; Trmrcic, J.; Moilliet, J. S. *Tetrahedron* **2006**, *62*, 7162–7167.
- (110) (a) Shilov, A. E.; Shul’pin, G. B. *Chem. Rev.* **1997**, *97*, 2879–2932. (b) Heyduk, A. F.; Zhong, H. A.; Labinger, J. A.; Bercaw, J. E. *Activation and Functionalization of CH Bonds*; ACS Symposium Series 885; American Chemical Society: Washington, DC, 2004. (c) Lersch, M.; Tilset, M. *Chem. Rev.* **2005**, *105*, 2471–2526.
- (111) Nizova, G. V.; Krevor, J. V. Z.; Kitaigorodskii, A. N.; Shulpin, G. B. *Bull. Acad. Sci. USSR, Div. Chem. Sci. (Engl. Transl.)* **1982**, *31*, 2480–2482.